doi.org/10.26434/chemrxiv.13146404.v1

# Data-science driven autonomous process optimization

Melodie Christensen, Lars Yunker, Folarin Adedeji, Florian Häse, Loic Roch, Tobias Gensch, Gabriel dos Passos Gomes, Tara Zepel, Matthew Sigman, Alan Aspuru-Guzik, Jason Hein

Submitted date: 02/11/2020 • Posted date: 02/11/2020



Citation information: Christensen, Melodie; Yunker, Lars; Adedeji, Folarin; Häse, Florian; Roch, Loic; Gensch, Tobias; et al. (2020): Data-science driven autonomous process optimization. ChemRxiv. Preprint. https://doi.org/10.26434/chemrxiv.13146404.v1

Autonomous process optimization involves the human intervention-free exploration of a range of pre-defined process parameters in order to improve responses such as reaction yield and product selectivity. Utilizing off-the-shelf components, we developed a closed-loop system capable of carrying out parallel autonomous process optimization experiments in batch with significantly reduced cycle times. Upon implementation of our system in the autonomous optimization of a palladium-catalyzed stereoselective Suzuki-Miyaura coupling, we found that the definition of a set of meaningful, broad, and unbiased process parameters was the most critical aspect of a successful optimization. In addition, we found that categorical parameters such as phosphine ligand were vital to determining the reaction outcome. To date, categorical parameter selection has relied on chemical intuition, potentially introducing an element of bias into the experimental design. In seeking a systematic method for the selection of a diverse set of phosphine ligands fully representative of the chemical space, we developed a strategy that leveraged computed molecular descriptor clustering analysis. This strategy allowed for the successful autonomous optimization of a stereoselective Suzuki-Miyaura coupling between a vinyl sulfonate and an arylboronic acid to selectively generate the E-product isomer in high yield.

# DATA-SCIENCE DRIVEN AUTONOMOUS PROCESS OPTIMIZATION

Melodie Christensen[1,2], Lars P.E. Yunker[1], Folarin Adedeji[2], Florian Häse[3,4,5,7,9], Loïc M. Roch[3,4,5,9], Tobias Gensch[6], Gabriel dos Passos Gomes[4,5,7], Tara Zepel[1], Matthew S. Sigman*[6], Alán Aspuru-Guzik*[3,4,5,7,8] and Jason E. Hein[1*,9]

[1]*Department of Chemistry, University of British Columbia, Vancouver, British Columbia V6T 1Z1, Canada.*
[2]*Department of Process Research and Development, Merck & Co., Inc., Rahway, NJ 07065, United States.*
[3]*Department of Chemistry and Chemical Biology, Harvard University, Cambridge, MA 02138, United States.*
[4]*Department of Chemistry, University of Toronto, Toronto, Ontario M5S 3H6, Canada.*
[5]*Department of Computer Science, University of Toronto, Toronto, Ontario M5T 3A1, Canada.*
[6]*Department of Chemistry, University of Utah, Salt Lake City, Utah 84112, United States.*
[7]*Vector Institute for Artificial Intelligence, Toronto, Ontario M5S 1M1, Canada.*
[8]*Canadian Institute for Advanced Research, Toronto, Ontario M5G 1Z8, Canada.*
[9]*ChemOS Sàrl, Lausanne, Vaud 1006, Switzerland.*

**Corresponding authors: Matthew S. Sigman sigman@chem.utah.edu, Alán Aspuru-Guzik aspuru@utoronto.ca, Jason E. Hein jhein@chem.ubc.ca*

## Abstract

Autonomous process optimization involves the human intervention-free exploration of a range of pre-defined process parameters in order to improve responses such as reaction yield and product selectivity. Utilizing off-the-shelf components, we developed a closed-loop system capable of carrying out parallel autonomous process optimization experiments in batch with significantly reduced cycle times. Upon implementation of our system in the autonomous optimization of a palladium-catalyzed stereoselective Suzuki-Miyaura coupling, we found that the definition of a set of meaningful, broad, and unbiased process parameters was the most critical aspect of a successful optimization. In addition, we found that categorical parameters such as phosphine ligand were vital to determining the reaction outcome. To date, categorical parameter selection has relied on chemical intuition, potentially introducing an element of bias into the experimental design. In seeking a systematic method for the selection of a diverse set of phosphine ligands fully representative of the chemical space, we developed a strategy that leveraged computed molecular descriptor clustering analysis. This strategy allowed for the successful autonomous optimization of a stereoselective Suzuki-Miyaura coupling between a vinyl sulfonate and an arylboronic acid to selectively generate the *E*-product isomer in high yield.

## Introduction

Recent advancements in computer science and automation technologies have led to the emergence of autonomous chemistry systems built on the premise of human intervention-free hypothesis generation and testing.[1] Autonomous workflows typically involve three key components: (1) a machine learning (ML) algorithm for hypothesis generation, (2) a robotic system for experimental execution, and (3) an online analytics platform for performance evaluation. The level of human intervention varies based on the degree of hardware and software integration among the key components. In a fully autonomous system, a "closed-loop" is achieved, where the scientist can define the search space, and then hit "go". Closed-loop applications have ranged from biologically active compound discovery[2] to materials development,[3] novel reaction scouting[4] and process optimization.[5]

Autonomous process optimization involves the human intervention-free exploration of a range of pre-defined process parameters to improve responses such as reaction yield, product selectivity and catalyst turnover number. The definition of a set of meaningful, broad, and unbiased process parameters is arguably the most critical aspect of a successful optimization. Work to date has focused on the multivariate optimization of continuous parameters such as temperature, stoichiometry and time; however, vital categorical parameters such as reagent, solvent or catalyst have rarely been incorporated. In fact, leading examples involving continuous and categorical parameter combinations have been limited to fewer than eight catalysts or ten solvents.[6] Furthermore, in these examples, categorical parameter selection was guided through chemical intuition, potentially introducing an element of bias into the experimental design. Thus, in our view, categorical parameter selection in the context of autonomous process optimization remains an unsolved challenge. We envisioned developing a more systematic method for the selection of a broad and diverse set of categorical parameters to fully represent the chemical space, driving more effective optimization campaigns.

Successful optimization also hinges on the identification of suitable automation equipment capable of effective experimental execution and analysis. Current research focuses heavily on custom-built continuous and segmented flow-reactor systems outfitted with online analytics for experimental execution. While these state-of-the-art systems have enabled the rapid multivariate optimization of several processes, examples have still been limited to the sequential execution of fast, homogeneous reactions amenable to flow reactors.[7] In this work, we expand the autonomous process optimization toolkit to include a broader set of reaction methodologies by integrating off-the-shelf robotic systems with online analytics to carry out parallel reaction loops in 96-well plates.

The final aspect of successful optimization is the selection of an effective ML algorithm. Recently, Bayesian optimization algorithms have gained traction in the in autonomous chemistry realm, leading to a number of successful optimization campaigns.[8] The advantage of Bayesian optimization is the implicit formulation of expected outcomes for all possible reaction conditions which are conditioned on all previous observations and constantly refined as soon as new observations become available. One example is the Phoenics[9] algorithm, a Bayesian optimizer developed for the global optimization of chemistry problems, with the capability to propose multiple parameter points in parallel. Another example is the Gryffin[10] algorithm, developed specifically for the identification of optimal choices for categorical parameters. Given our interest in the autonomous optimization of categorical and continuous parameters in tandem through the execution of parallel reaction loops, we combined the Phoenics and Gryffin optimization strategies to satisfy both requirements.

We identified a stereoselective Suzuki-Miyaura cross-coupling reaction that would benefit from a tandem categorical and continuous parameter optimization (Figure 1).[11] Typically, Suzuki-Miyaura cross-couplings of vinyl halides or sulfonates proceed with retention of the olefin bond geometry, but in this example, vinyl sulfonate **1-*E*** undergoes stereoinversion under ligand-free and electron-rich dialkylbiaryl phosphine-mediated palladium catalysis to generate product ***2-Z***. In contrast, stereoinversion is partially suppressed using ferrocenyl bisphosphine-mediated palladium catalysis, facilitating the selective formation of product ***2-E***. Thus, stereoselectivity in this system appears to be influenced by both the phosphine ligand selection and stoichiometry.[12] Importantly, traditional phosphines preferred in Suzuki couplings, such as dialkylbiaryl phosphine ligands,[13] appear to facilitate the undesired steroinversion pathway. Finally, with reaction completion times in the order of two hours, this system is not amenable to flow reactors due to impractically long residence times.

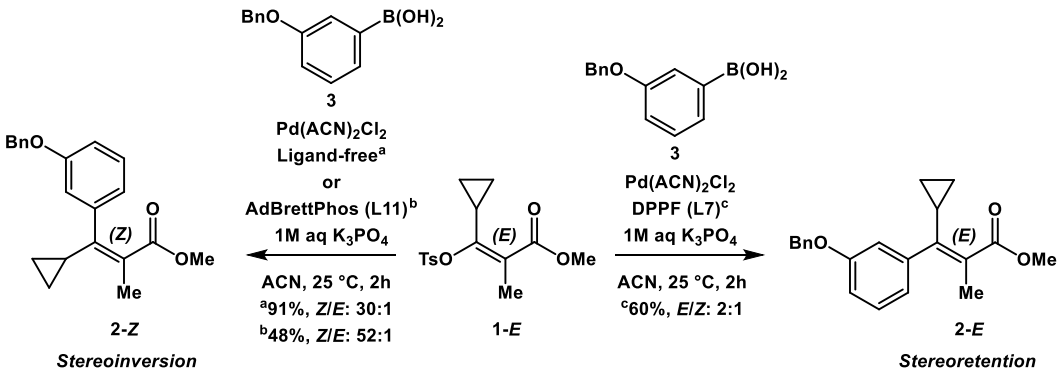


**Figure 1. Phosphine ligand and reaction condition influence on a palladium-catalyzed stereoselective Suzuki-Miyaura coupling to generate the stereoinversion (2-*Z*) or stereoretention product (2-*E*).**
[a] Conditions: 10 µmol **1-*E***, 1 µmol 1,3,5-trimethoxybenzene, 20 µmol **3**, 0.4 µmol $Pd(ACN)_2Cl_2$, 30 µmol $K_3PO_4$ (0.5M aq) in ACN (0.05M), 2 h at 25 °C.
[b,c] Conditions: 10 µmol **1-*E***, 1 µmol 1,3,5-trimethoxybenzene, 11 µmol **3**, 0.2 µmol $Pd(ACN)_2Cl_2$, 0.4 µmol **L**, 30 µmol $K_3PO_4$ (0.5M aq) in ACN (0.05M), 2 h at 25 °C. Ligand structures are provided in Figure 3.

Our goal was to improve the yield of stereoretention product ***2-E*** through an autonomous optimization campaign by exploring a selection of phosphines and continuous process parameters in tandem. We employed a Chemspeed SWING robotic system for the experimental execution of parallel reaction loops in batch and employed the Phoenics and Gryffin algorithms for the proposal of parallel combinations continuous and categorical process parameter selections. Recognizing the impact of phosphine selection on the optimization outcome, we employed a variety of categorical parameter selection strategies, including chemical intuition and computed molecular descriptor clustering of 365 commercially available phosphines.[14] Here, we discuss the advantages and limitations of each phosphine selection strategy and their impacts on this challenging optimization problem.

# Results

## Establishing a closed-loop system

The establishment of a closed-loop system required the integration of three main components: (1) ChemOS,[15] the experimental scheduler for coordination of experiments proposed by the ML algorithms (Phoenics and Gryffin), (2) Chemspeed SWING, the robotic system for automated experimental set-up, and (3) Agilent 1100, the HPLC-UV system for measurement of the experimental outcomes (Figure 2). The only hardware customization required was the integration of the Agilent HPLC-UV system with the Chemspeed SWING robotic platform. This integration was accomplished through the installation of an HPLC valve on the Chemspeed robot deck and incorporation of relay switches for triggering chromatographic resolution and photodiode array detection.[16] The next step was to establish automated data flow from the experimental scheduler to the robot, and from the online analytical system back to the experimental scheduler for the ML algorithm to interpret results and propose subsequent experiments. In lieu of developing a complex Application Programming Interface (API) among the three software components (ChemOS, Chemspeed Autosuite, and Agilent Chemstation), we opted to develop a lightweight Python framework for data transfer between these components. The script translated ChemOS parameter suggestions into stock mixture dispense volumes, calculated product assay yields from HPLC peak area ratios to an internal standard and reported experimental measurements back to ChemOS.

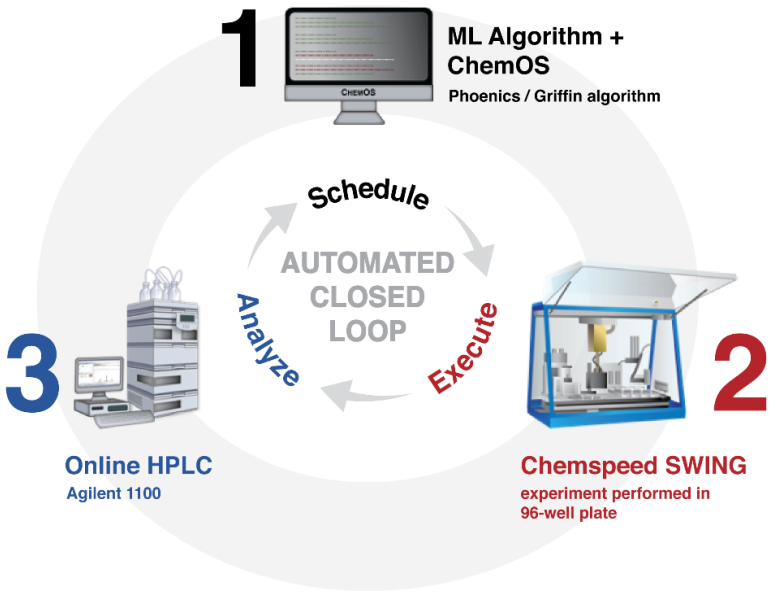


**Figure 2. Closed-loop system for autonomous optimization in batch. The three main components to enable this closed-loop include (1) ChemOS to coordinate experiments and data-driven approaches, (2) Chemspeed SWING for automated experimental setup, and (3) Agilent 1100 to characterize the experimental outcomes.**

## Defining the process parameters and optimization objectives

A set of categorical and continuous parameters was selected for potential impact on the reaction outcome, including phosphine ligand, phosphine to palladium ratio, palladium loading, arylboronic acid equivalents, and reaction temperature (Table 1). Upper and lower bound selection for each continuous parameter was guided by chemical intuition but also designed to be sufficiently broad to explore a diverse set of responses. Ligand set selections varied from 12 up to 23 ligands, depending on the selection strategy (see below). The ML algorithms (Phoenics and Gryffin) were configured to maximize the yield of the *E*-product, minimize the yield of the *Z*-product, minimize the palladium loading, and minimize the arylboronic acid equivalents, in that order (Table 1). Each objective was configured with a 10 % relative threshold that would only consider the next objective once that threshold had been achieved. This multi-objective optimization, or Pareto optimization design, was made possible through the implementation of the scalarizing function Chimera.[17]

**Table 1. Process parameters and optimization objectives**

| **Parameter** | **Type** | **Range** | **Unit** |
|---|---|---|---|
| Phosphine ligand (P ligand) | Categorical | 12 – 23 | Number of ligands |
| Phosphine to palladium ratio (P/Pd) | Continuous | 0.5 – 4.0 | ratio |
| Palladium loading (Pd mol%) | Continuous | 1.0 – 5.0 | mol % |
| Arylboronic acid equivalents (ArBA equiv)* | Continuous | 1.0 – 2.0 | equivalents |
| Reaction temperature (Rxn temp) | Continuous | 10 – 40 | °C |
| **Response** | **Objective** | **Priority** | **Unit** |
| *E*-product assay yield (*E*-PR AY) | Maximize | First | mol % |
| *Z*-product assay yield (*Z*-PR AY) | Minimize | Second | mol % |
| Palladium loading (Pd mol%) | Minimize | Third | mol % |

Arylboronic acid equivalents (ArBA equiv)* Minimize Fourth equivalents
*Note: The arylboronic acid equivalents parameter and response was removed from the experimental design upon expanding the search space from 12 to 23 ligands.

## Designing the automation workflow

Given the broad search space, a reasonable number of reactions for an autonomous optimization campaign was determined to reside between 120 and 192, depending on the number of ligands under evaluation. Full conversion in this Suzuki-Miyaura coupling is typically achieved within two hours under the median values of the continuous parameter ranges defined above. Thus, if the maximum number of 192 consecutive reactions were carried out sequentially, the optimization campaign would take 16 days to complete. This lengthy duration would serve to obviate the benefits of autonomous optimization, and correspondingly, necessitated parallelization of the reactions. Therefore, the reactions were parallelized into loops of eight, allowing for a 192-reaction campaign to be completed within 24 loops over a more reasonable time period of four days. Conditions for the first loop of eight reactions were selected randomly by the ML algorithm. Subsequent conditions were determined autonomously by Phoenics and Gryffin as analytical results were returned, following a data-driven strategy. ChemOS, the experimental scheduler, parallelized the suggested reactions for the Chemspeed SWING system to dispense and initiate in 15-minute intervals. Analytical samples were also aliquoted and acquired in 15-minute intervals, at the endpoint of each reaction.

## Trial runs and experimentally-derived constraints for the optimization strategy

Trial runs unveiled two instrument constraints that necessitated further enhancements of the optimization strategy. The first constraint involved the need to fix the reaction temperature across each loop of eight reactions given that these reactions were designed to be carried out within the same reactor block and timeframe. In order to accommodate this constraint, the capabilities of the Phoenics and Gryffin optimization strategies were extended to facilitate optimization with process constraints following the idea of a previously introduced basic process-constrained Bayesian optimization algorithm (pc-BO(basic)).[18] This extension allowed the suggestion of a total of eight different experiments where the temperature was fixed across one loop. The second instrument constraint was the inability of the Chemspeed robot to execute sub-microliter dispenses accurately; thus, the Python script was augmented to round calculated dispense volumes to the microliter level and update the suggested parameters with the executed parameters prior to returning analytical results to ChemOS. These enhancements allowed for the successful application of an algorithm in a real-world experimental setting.

## Autonomous optimization with ligands selected through chemical intuition

Initial ligand selection was carried out through chemical intuition around phosphines with the potential to accelerate palladium-catalyzed cross-couplings[19] (here, chemical intuition refers to insight arising from a combination of literature precedent and hands-on experience). Twelve ligands were selected, including trialkyl, triaryl, ferrocenyl and dialkylbiaryl phosphines. These ligands were evaluated in combination with four continuous parameters, including phosphine ligand, phosphine to palladium ratio, palladium loading, arylboronic acid equivalents, and reaction temperature. The optimization campaign was carried out in fifteen loops of eight reactions, totaling 120 autonomous iterations carried out over 60 hours. This first campaign resulted in conditions to access product **2-*E*** in 65% yield and 2:1 *E*/*Z* selectivity upon 118 iterations, under Pd-**L7** catalysis (Figure 3). It was also noted that the optimizer dedicated a higher number of iterations to **L7** (DPPF), the top-performing ligand. Although this optimization should be viewed as

successful, improvements to product **2-*E*** yields from our initial conditions were nominal (compared to 60% yield and 2:1 *E*/*Z* selectivity as shown in Figure 1). This nominal improvement was attributed to ligand bias resulting from chemical intuition-based selection, thus, we embarked upon the exploration of a broader set of ligands to access **2-*E*** in higher yield and selectivity.

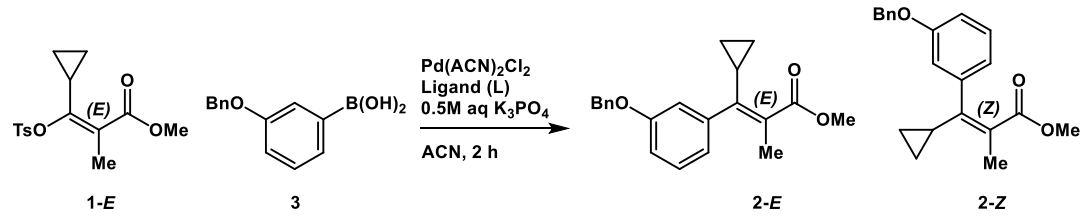


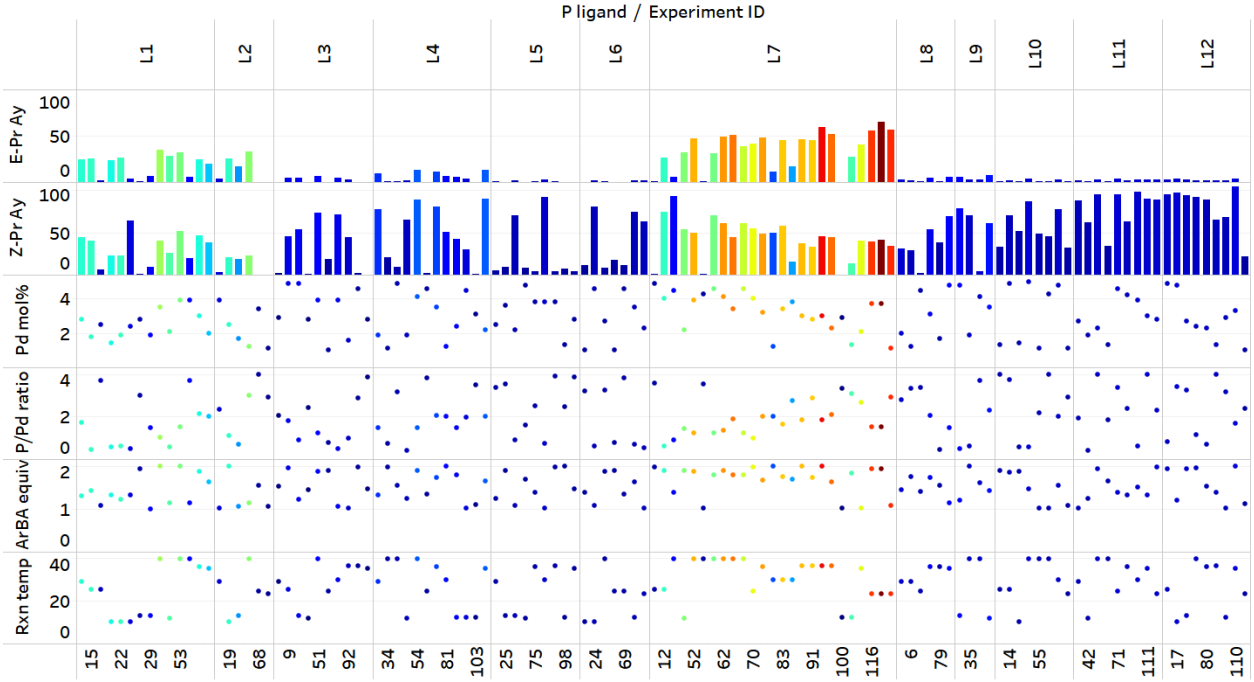


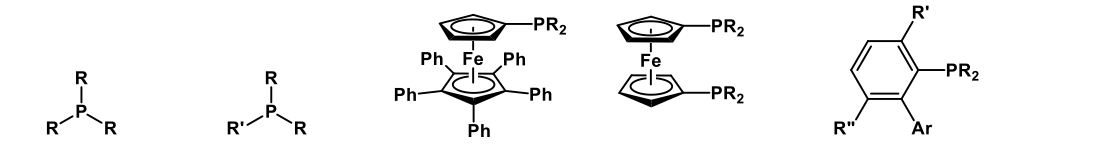


L1: $PPh_3$ R = Ph
L2: $PoTol_3$ R = Tol
L3: $PtBu_3$ R = tBu

L4: AtaPhos
R = tBu R'= 4-$NMe_2$-Ph
L5: MorDalPhos
R = Ad R'= 2-Mor-Ph

L6: QPhos R = tBu

L7: DPPF R = Ph
L8: DTBPF R = tBu

Ar = 2,4,6-$iPr_3$-Ph
L9: XPhos R = Cy R'/R"= H
L10: BrettPhos R = Cy R'/R"= OMe
L11: AdBrettPhos R= Ad R'/R"= OMe
L12: RockPhos R = tBu R'= OMe R"= Me

**Figure 3. Parameters and results of optimization with ligands selected through chemical intuition (campaign 1).**

Conditions: 10 µmol **1-*E***, 1 µmol 1,3,5-trimethoxybenzene, 10 - 20 µmol **3**, 0.1 - 0.5 µmol $Pd(ACN)_2Cl_2$, 0.05 - 2 µmol **L**, 30 µmol $K_3PO_4$ (0.5M aq) in ACN (0.05M), 2 h at 10 - 40 °C.

## Autonomous optimization with ligands selected through computed molecular features

To this end, we sought a systematic method for the selection of a diverse set of phosphines for autonomous evaluation. A particularly attractive approach would leverage computed molecular features of phosphines as these have been applied to reaction optimization through predictive modeling.[20] In our current study, 365 commercially available monodentate phosphines were used to define the chemical space (the focus was limited to monodentate phosphines in order to more effectivity control the ligation state of palladium). For each phosphine, features were obtained by computing molecular properties for a representative set of conformers using DFT. Then, k-means clustering was carried out on the first four principal components of this descriptor set to divide the chemical space into 24 regions. A single compound was selected from each cluster for experimental evaluation based on additional considerations such as availability in the Merck phosphine library, price, and anticipated stability (Figure 4).[21] One cluster contained ligands that were deemed too challenging to implement; therefore, candidates from this cluster were not included in the experimental design.[22]

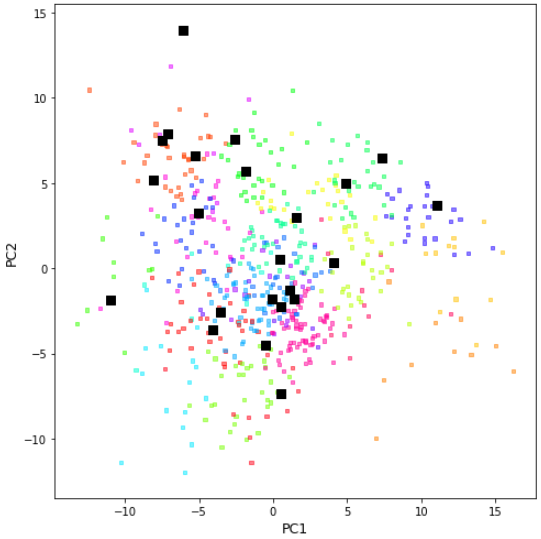


**Figure 4. K-means clustering on the first four principal components of the molecular descriptor set for 365 commercial monodentate phosphines. The chemical space is represented by a two-dimensional plot of the first two principal components.**
Note: Each cluster is represented by color and highlighted boxes indicate selected candidates.

Investigation of a larger ligand set necessitated the expansion of the optimization campaign to 24 loops of eight reactions, totaling 192 autonomous iterations executed over 96 hours (16 of these reactions were designated as test reactions to test for reproducibility, accuracy and precision). In addition, the larger ligand set also drove the removal of the arylboronic acid equivalents parameter and response from the experimental design. This second campaign resulted in the identification of optimal conditions to access product **2-*E*** in 73% yield and 3:1 *E*/*Z* selectivity upon 161 iterations, using **L30** as the ligand (Figure 5a). Given that the ML algorithm had no information to bias the search, and that ligand selection was unbiased, the improved stereoselectivity of 3:1 highlights the potential of our novel optimization technology. As in the first campaign, the algorithm dedicated a significant portion of iterations to the top-performing ligand; previously **L7** (DPPF), now **L30** (PhSPhos). Additional high-performing ligands also fell under the triaryl phosphine category, with both electron-rich (**L20**, **L21**) and electron-poor (**L26**) triaryl phosphines proving effective. Surprisingly, ligands with significant structural similarity to **L30** (PhSPhos), including **L28** and **L31**

(SPhos), did not selectively yield **2-*E***, presumably due to the presence of two electron-rich cyclohexyl substituents.

A deeper look into the influence of the continuous parameters on the yield of product **2-*E*** (Figure 5b) revealed that phosphine to palladium ratios within the center of the studied range provided optimal outcomes. In fact, phosphine to palladium ratios near the upper and lower bound values resulted in significant declines in yields. Conversely, performing the reaction at temperatures near the upper bound of the evaluated range proved most effective in driving product formation. Finally, and unsurprisingly, higher palladium loadings resulted in improved product **2-*E*** yields; however, the algorithm appeared to explore a bimodal distribution of palladium loading, focusing on regions close to 1.5 mol% and 3.5 mol%, landing at an optimum of 3.7 mol%. Although we are currently unable to interpret this bimodal exploration behavior, we are pleased to observe that the algorithm does not default to maximizing to upper bound values when presented with potentially linear trends.

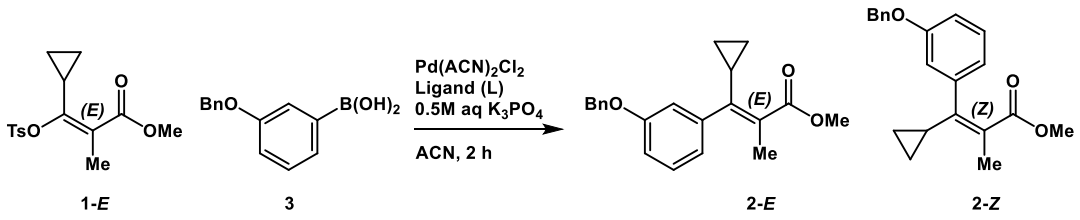


**a.**

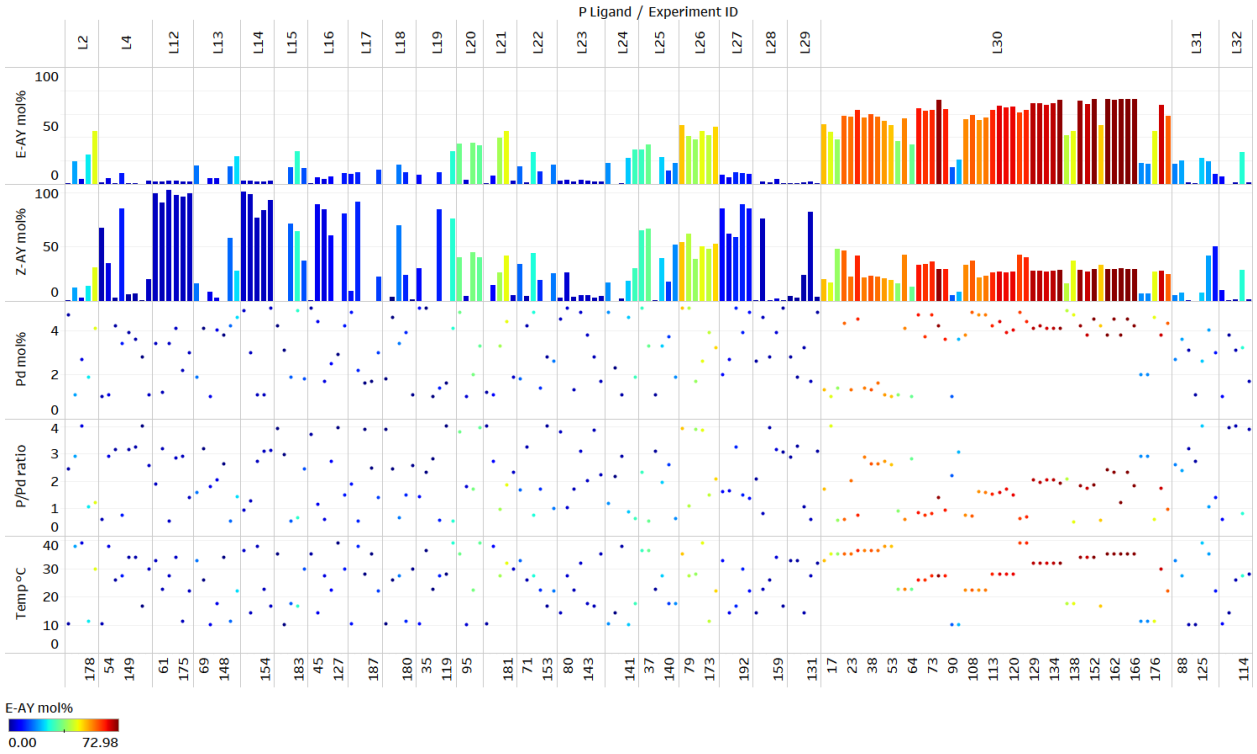

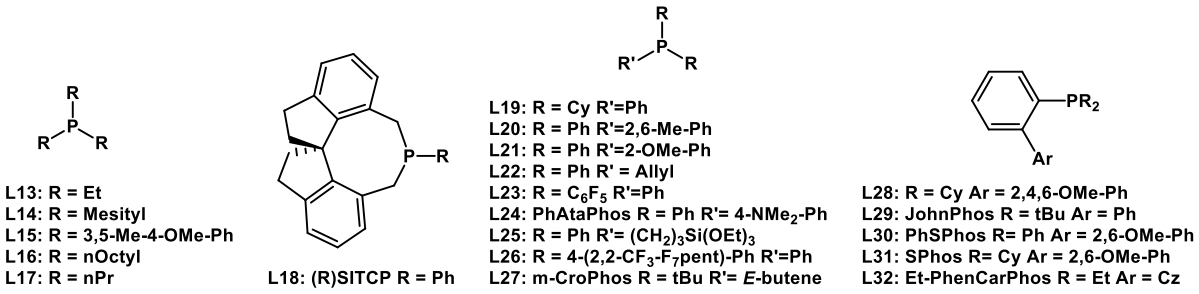


**b.**

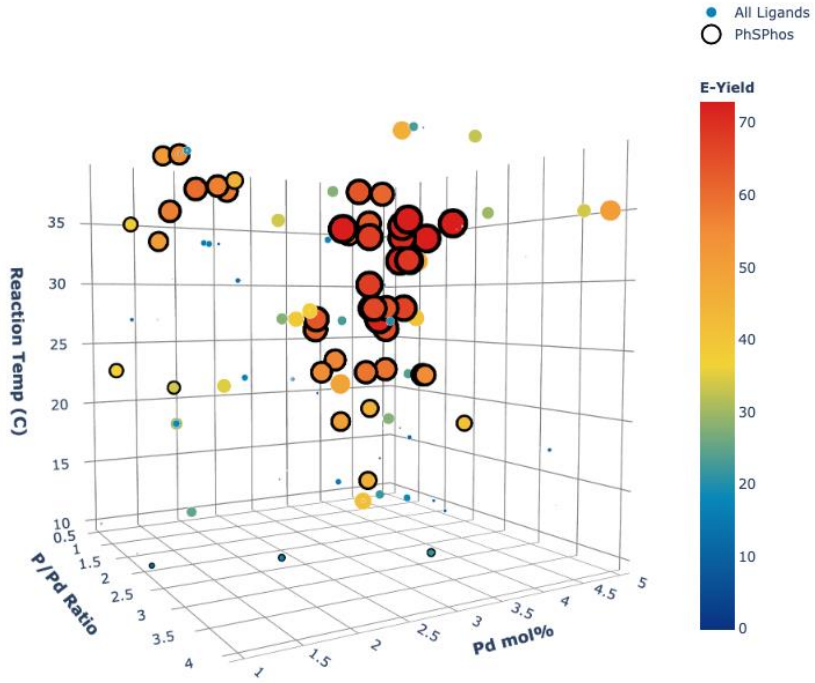


**Figure 5a. Parameters and results of optimization with ligands selected through descriptor clustering (campaign 2). 5b. 3D visualization of continuous parameters vs. *E*-product yield (campaign 2). PhSPhos results are outlined; all other ligand results are not outlined.**

Conditions: 10 µmol **1-*E***, 1 µmol 1,3,5-trimethoxybenzene, 15 µmol **3**, 0.1 - 0.5 µmol $Pd(ACN)_2Cl_2$, 0.05 - 2 µmol **L**, 30 µmol $K_3PO_4$ (0.5M aq) in ACN (0.05M), 2 h at 10 - 40 °C.

Comparison of the optimization results from the two campaigns superimposed on the monodentate phosphine ligand space clearly demonstrates the advantage of systematic ligand selection over chemical intuition-based ligand selection (Figure 6). A wider range of product **2-*E*** yields were observed through the systematic exploration of a diverse set of ligands, ultimately leading to the discovery of **L30** as a superior ligand. This is likely due to the challenging nature of the stereoselective Suzuki-Miyaura coupling under evaluation, where selectivity appears to be driven by ligand selection through a poorly understood mechanism, driving the need for empirical ligand exploration.

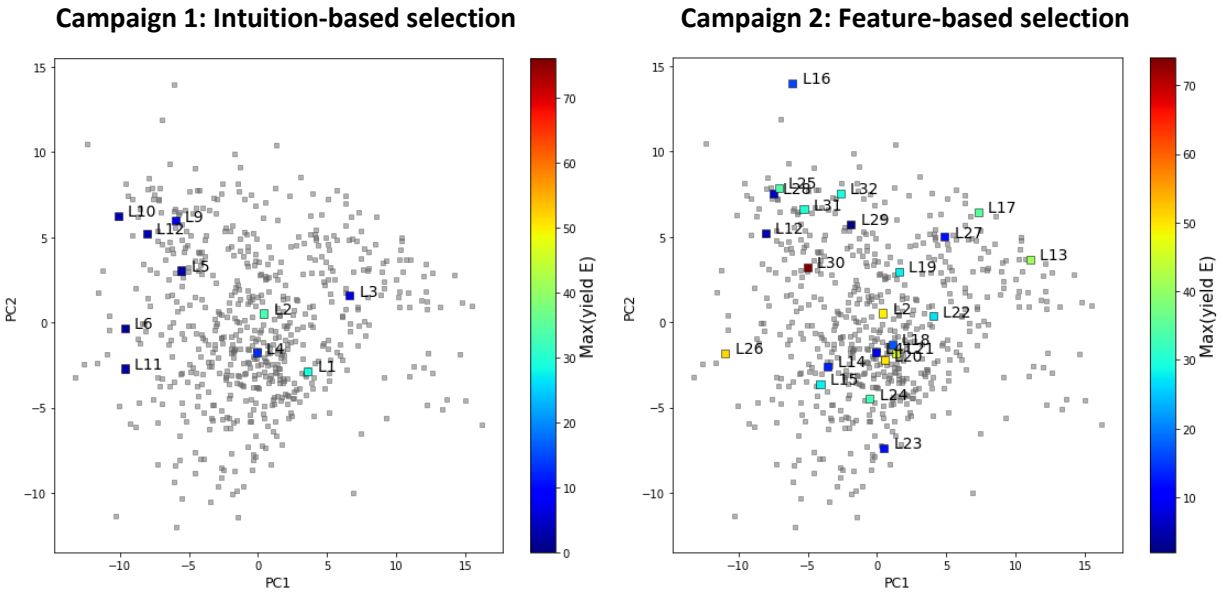


**Figure 6. The maximum yield of 2-*E* obtained for each monodentate ligand explored in campaigns 1 and 2 as a function of the monodentate phosphine ligand space.**

At this stage, the only question that remained unanswered was whether the algorithm's optimization performance could be improved if ligands were parametrized within the algorithm instead of being treated as black-box parameters. We hypothesized that the utilization of computed molecular descriptors as a means for the algorithm to relate among ligands could accelerate convergence. We therefore manually selected 15 from of the hundreds of descriptors utilized in ligand selection and carried out a third 192-iteration optimization campaign.[23] We found that a similar optimum was reached, accessing product **2-*E*** in 74% yield and 3:1 *E*/*Z* selectivity upon iteration 159, again under Pd-**L30** catalysis. Surprisingly, the algorithm did not appear to converge as clearly as in the previous campaign because fewer iterations focused on the top ligand (**L30**) and, in fact, a high number of iterations focused on unproductive ligands.[24] This observation may be attributed to some form of unproductive bias introduced by the selected set of descriptors, solidifying that an unbiased ligand section was critical to the success of this optimization.

## Follow-up experiments with *E*-selective ligands identified through predictive modeling

With two 192-iteration data sets in hand, various modeling strategies were employed to predict additional phosphines that could also promote *E*-selectivity.[25] We found that a reasonable multivariate linear regression model (MLR) was generated, and multiple ligands with the potential for *E*-selectivity were proposed.[26] Manual experiments employing six of the predicted ligands were carried out utilizing the optimal conditions identified from autonomous optimization to measure the selectivity outcome. Additionally, **L30** was employed in a control experiment. Upon experimental execution, we were pleased to find that experimental results agreed with the predictions (Figure 7). Although Pd-**L30** still offered the highest olefin **2-*E*** yield and E/Z ratio, two ligands (**L34**, **L36**) out of six were identified that surpassed the 50% threshold for product **2-*E*** yield, meaning that one-third of the ligands proposed offered *E*-selectivity. This result is a significant improvement over the ligand set identified in the initial clustering analysis, where employment of only one-twelfth of the ligands surpassed the 50% yield threshold for generating

product **2-*E***. It is important to note that the newly identified *E*-selective ligands are structurally distinct from **L30** and, thus, it would have been unlikely to arrive at these selections through chemical intuition.

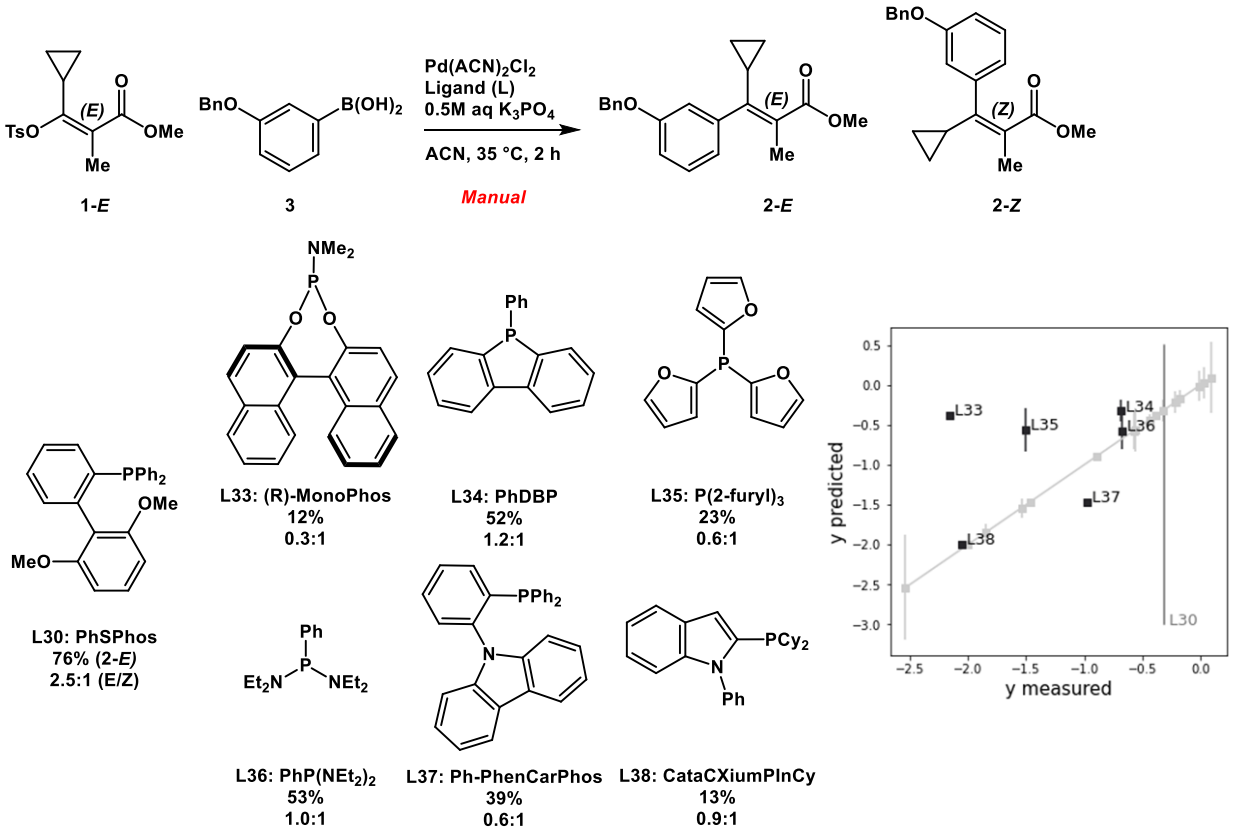


**Figure 7. Manual experiments under optimized conditions with predicted *E*-selective ligands.**
Note: y is the ln of the highest yield of **2-*E*** per ligand in any experiment.
Conditions: 10 µmol **1-*E***, 1 µmol 1,3,5-trimethoxybenzene, 15 µmol **3**, 0.4 µmol $Pd(ACN)_2Cl_2$, 0.9 µmol **L**, 30 µmol $K_3PO_4$ (0.5M aq) in ACN (0.05M), 2 h at 35 °C.

## Discussion

We have demonstrated the human-intervention free multivariate optimization of a stereoselective Suzuki-Miyaura coupling in batch through the autonomous evaluation of a large phosphine ligand set and continuous parameters in tandem. This success was accomplished through a series of technological advances. First, the implementation of a robotic system capable of carrying out parallel experiments with online analytics significantly reduced cycle times. Second, the development of seamless communication between the ML algorithm and robotic hardware established a closed-loop system. Third, the incorporation of Bayesian ML algorithms, here Phoenics and Gryffin, facilitated tandem categorical and continuous parameter optimization. Finally, the employment of computed molecular features enabled the systematic and unbiased definition of the phosphine ligand search space. The application of these advances resulted in the rapid identification of optimal conditions and ligand clusters to maximize the yield of product **2-*E***.

It is relevant to ask what advantage autonomous optimization offers over more well-established technologies such as HTE (high-throughput experimentation) or DOE (design of experiments). Although we view algorithmic optimization as a complementary technology, we also believe its advantage lies in the multivariate optimization of categorical and continuous parameters in tandem within the fewest

number of iterations. To elaborate on this point, a theoretical comparison among the technologies in the context of this Suzuki-Miyaura optimization is warranted. The goal of this optimization was to evaluate 23 categorical and three continuous parameters in tandem to maximize the yield of product **2-*E***. In our studies, we observed that the yield of product **2-*E*** followed a bell-shaped distribution with respect to one of the continuous parameters, phosphine to palladium ratio. In an HTE or DOE paradigm, studying the lower, center and upper bound values of each continuous parameter with each ligand would have resulted in 621 experiments, much higher than the number of experiments reported in our successful autonomous optimization (192 experiments). DOE factorial designs with fewer experiments could have been implemented, but this approach would have sacrificed center points, in this case leading to the potential to miss the global optimum of phosphine to palladium ratio. Thus, at least in the context of this optimization, the autonomous approach theoretically proved most efficient in the identification of the global optimum within the fewest number of iterations.

The autonomous optimization approach can easily be replicated to solve a multitude of multivariate process optimization problems. Once widely adopted, the technology has the potential to empower modern-day chemists to shift their focus away from routine experimental execution and towards higher-complexity problem-solving. Areas for future improvement include further extensions of algorithmic schemes to facilitate process-constrained batch optimization as well as enhancements to multivariate data analysis to drive a better understanding of reaction trends, in essence, to learn what the algorithm learned.

# Methods

## Instrumentation

Autonomous optimization experiments were executed using a Chemspeed SWING robotic system equipped with a four-needle dispense head and four 1 mL syringe pumps to enable accurate dispenses at low volumes. Slurry dispensing was enabled through 0.8 mm needle inner diameters. Agitation was carried out through an integrated custom V&P scientific 2-position tumble stirring module and temperature control was achieved through an integrated Huber Unistat chiller with temperature feedback control. Online HPLC analysis was carried out through an integrated Agilent 1100 HPLC equipped with a photodiode array detector and a custom sampling valve installed on the robot deck.

## Automation of data flow

ChemOS was utilized as the scheduler that packaged proposed experiments from the machine learning algorithm into batches of eight for execution by the Chemspeed SWING robotic module. Communication of ChemOS with the Chemspeed SWING robot and Agilent HPLC was established through a lightweight Python tool. This script parsed experimental parameters proposed by ChemOS, calculated dispense volumes based on stock solution concentrations, and wrote those volumes to a CSV file actively being monitored by the Chemspeed Autosuite software. Upon automated experimental execution and subsequent HPLC analysis, this script also parsed Agilent HPLC report files for peak area counts to and calculated product yields based on predetermined response factors, which were then reported back to ChemOS for interpretation and proposal of new experimental parameters.

## Experimental planning algorithms

The ML algorithms used for experiment planning in this study, Phoenics and Gryffin, leverage fundamental concepts from Bayesian optimization in combination with kernel density estimation. Bayesian

optimization is an approach to global optimization for applications where the evaluation of a single parameter point is highly time or resource demanding. While several formulations exist, Bayesian optimization follows a two-step strategy to suggest parameter points for future evaluation: (1) constructing a statistical approximation to the considered experiment based on collected measurements, and (2) locating parameter points for which the approximation predicts promising performance. Phoenics and Gryffin construct the statistical approximation based on kernel density estimates of evaluated parameters and suggest promising parameter points with an explicit balance of exploitative and explorative sampling behavior with native support for batch optimization.

## Automated experimental procedure

*General:* Stock solutions or slurries were prepared manually in anhydrous ACN under $N_2$ atmosphere and placed on the robot deck for autonomous execution. Two fluoropolymer and PFA mat-sealed 96-well metal blocks with 1 mL glass vial inserts were equilibrated at the designated reaction temperature under 20 psig of $N_2$ with 500 rpm agitation.

*Representative procedure for test reactions:* In campaigns involving 192 iterations, eight wells from each 96-well reaction block were dedicated to standard reactions to test for reproducibility. To each well was dispensed $Pd(ACN)_2Cl_2$ (0.25 µmol, 25 µl of 0.01 M stock solution), and **L2** ($PoTol_3$) (0.38 µmol, 19 µl of 0.02 M stock mixture), followed by 7 min of age time. Then, *E*-tosylate **1-*E*** (10 µmol) with 1,3,5-trimethoxybenzene (1 µmol) was dispensed (20 µl of 0.5 M/ 0.05 M stock solution), followed by (3-(benzyloxy)phenyl)boronic acid **3** (15 µmol, 30 µl of 0.5 M stock solution in degassed ACN 5% $H_2O$), followed by anhydrous ACN (106 µl) to ensure a total organic solvent volume of 200 µl. Then, a dispense of degassed aqueous $K_3PO_4$ (30 µmol, 60 µl of 0.5 M stock solution) was carried out to initiate the reaction. This procedure was executed sequentially for each well within a loop of eight replicates in 15-minute intervals. Each replicate was time stamped individually, aged for 120 min, and sampled for online analysis.

*Representative procedure for optimization reactions:* In campaigns involving 192 iterations, 88 wells from each 96-well reaction block were dedicated to the optimization reactions. To each well was dispensed $Pd(ACN)_2Cl_2$ (0.1 - 0.5 µmol, 10 - 50 µl of 0.01 M stock solution), and phosphine ligand (0.05 - 2.0 µmol, 3 - 100 µl of 0.02 M stock mixture), followed by 7 min of age time. Then, E-tosylate **1-*E*** (10 µmol) with 1,3,5-trimethoxybenzene (1.0 µmol) was dispensed (20 µl of 0.5 M/ 0.05 M stock solution), followed by (3-(benzyloxy)phenyl)boronic acid **3** (15 µmol, 30 µl of 0.5 M stock solution in degassed ACN 5% $H_2O$), followed by anhydrous ACN (0 - 138 µl) to ensure a total organic solvent volume of 200 µl. Then, a dispense of degassed aqueous $K_3PO_4$ (30 µmol, 60 µl of 0.5 M stock solution) was carried out to initiate the reaction. This procedure was executed sequentially for each well within a loop of eight experiments in 15-minute intervals. Each reaction was time stamped individually, aged for 120 min, and sampled for online analysis.

*Sampling and analysis:* Two polypropylene 96-well collection blocks sealed with a silicone mats were manually prefilled with 800 µl of acetonitrile 10% aqueous pH 3.5 ammonium formate buffer and placed on the robot deck. Upon reaching the reaction end point at 120 min, 10 ul of reaction mixture was aliquoted and dispensed into the 800 ul quench solution in the collection block. Upon needle-mixing, 40 ul of quenched sample from the collection block was aliquoted and injected to the on-deck sampling valve outfitted with a 5 µl loop. The valve was automatically switched to transfer the sample to the Agilent 1100 HPLC for analysis.

## Phosphine descriptor calculations and predictive modeling

Electronic and steric descriptor calculations for 365 commercially available phosphine ligands have been

described previously.[27] Additionally, employed predictive modeling strategies surrounding parametrized phosphines have also been described previously.[28]

## Conflicts of interest

There are no conflicts of interest to declare.

## Acknowledgements

The authors are grateful to the Defense Advanced Research Projects Agency (DARPA) for funding this project under the Accelerated Molecular Discovery Program under Cooperative Agreement No. HR00111920027, dated August 1, 2019. Additional financial support for this work was provided by the University of British Columbia, the Canadian Foundation for Innovation (CFI-35883), and NSERC (RCPIN-2016-04613). We thank *Compute Canada* for computational resources. Part of DFT calculations were performed on the *niagara* supercomputer at the SciNet HPC Consortium. SciNet is funded by the Canada Foundation for Innovation; the Government of Ontario; Ontario Research Fund - Research Excellence; and the University of Toronto. We also acknowledge the Department of Navy award (N00014-19-1-2134) issued by the Office of Naval Research. The United States Government has a royalty-free license throughout the world in all copyrightable material contained herein. Any opinions, findings, and conclusions or recommendations expressed in this material are those of the authors and do not necessarily reflect the views of the Office of Naval Research. A. A.-G. thanks Anders G. Frøseth for his generous support. A. A.-G. also acknowledges the generous support of Natural Resources Canada and the Canada 150 Research Chairs program. M. S. S. thanks the NSF under the CCI Center for Computer Assisted Synthesis (CHE-1925607) for support. M.C. gratefully acknowledges the department of Process R&D at Merck & Co., Inc., Kenilworth, NJ, USA for student research support. F.H., L.M.R., and A. A.-G. were supported by the Tata Sons Limited - Alliance Agreement (A32391). G.P.G. gratefully acknowledges the Natural Sciences and Engineering Research Council of Canada (NSERC) for the Banting Postdoctoral Fellowship. The authors would also like to thank Dr. Rebecca T. Ruck, Dr. Alexandra C. Sun and Paloma Prieto for their assistance with the manuscript.

---

[1] Jensen, K. F., Coley, C. W. & Eyke, N. S. Autonomous discovery in the chemical sciences part I: Progress. *Angew. Chem. Int. Ed.* anie.201909987 (2019); Coley, C. W., Eyke, N. S. & Jensen, K. F. Autonomous discovery in the chemical sciences part II: Outlook. *Angew. Chem. Int. Ed.* anie.201909989 (2019); Häse, F., Roch, L. M. & Aspuru-Guzik, A. Next-Generation Experimentation with Self-Driving Laboratories. *Trends Chem.* **1,** 282–291 (2019); Stein, H. S. & Gregoire, J. M. Progress and prospects for accelerating materials science with automated and autonomous workflows. *Chem. Sci.* **10,** 9640–9649 (2019).

[2] Desai, B. *et al.* Rapid discovery of a novel series of Abl kinase inhibitors by application of an integrated microfluidic synthesis and screening platform. *J. Med. Chem.* **56,** 3033–3047 (2013); Weber, L., Wallbaum, S., Broger, C. & Gubernator, K. Optimization of the Biological Activity of Combinatorial Compound Libraries by a Genetic Algorithm. *Angew. Chem. Int. Ed.* **34,** 2280–2282 (1995).

[3] Burger, B. *et al.* A mobile robotic chemist. *Nature* **583,** 237–241 (2020); MacLeod, B. P. *et al.* Self-driving laboratory for accelerated discovery of thin-film materials. *Sci. Adv.* **6,** eaaz8867 (2020); Porwol, L. *et al.* An Autonomous Chemical Robot Discovers the Rules of Inorganic Coordination Chemistry without Prior Knowledge. *Angew. Chem. Int. Ed.* anie.202000329 (2020); Gongora, A. E. *et al.* A Bayesian experimental autonomous researcher for mechanical design. *Sci. Adv.* **6,** eaaz1708 (2020); Langner, S. *et al.* Beyond Ternary OPV: High-Throughput Experimentation and Self-Driving Laboratories Optimize Multicomponent Systems. *Adv. Mater.* **32,** 1907801 (2020); Tabor, D. P. *et al.* Accelerating the discovery of materials for clean energy in the era of smart automation. *Nat. Rev. Mater.* **3,** 5–20 (2018); Nikolaev, P. *et al.* Autonomy in materials research: A case study in carbon nanotube growth. *npj Comput. Mater.* **2,** 1–6 (2016).

[4] Granda, J. M., Donina, L., Dragone, V., Long, D. L. & Cronin, L. Controlling an organic synthesis robot with machine learning to search for new reactivity. *Nature* **559,** 377–381 (2018); Sans, V. & Cronin, L. Towards dial-a-molecule by integrating continuous flow, analytics and self-optimisation. *Chem. Soc. Rev.* **45,** 2032–2043 (2016); Sans, V., Porwol, L., Dragone, V. & Cronin, L. A self optimizing synthetic organic reactor system using real-time in-line NMR spectroscopy. *Chem. Sci.* **6**, 1258–1264 (2015).

[5] Mateos, C., Nieves-Remacha, M. J. & Rincón, J. A. Automated platforms for reaction self-optimization in flow. *React. Chem. Eng.* **4,** 1536–1544 (2019); Clayton, A. D. et al. Algorithms for the self-optimisation of chemical reactions. *React. Chem. Eng.* **4**, 1545–1554 (2019); Bédard, A.-C., Adamo, A., Aorh, K. C., Russell, M. G.; Bedermann, A. A., Torosian, J., Yue, B., Jensen, K. F. & Jamison, T. F. Reconfigurable system for automated optimization of diverse chemical reactions. *Science* **361**, 1220–1225 (2018); Baumgartner, L. M., Coley, C. W., Reizman, B. J., Gao, K. W. & Jensen, K. F. Optimum catalyst selection over continuous and categorical process variables with a single droplet microfluidic reaction platform. *React. Chem. Eng.* **3,** 301–311 (2018); Cortés-Borda, D. *et al.* An Autonomous Self-Optimizing Flow Reactor for the Synthesis of Natural Product Carpanone. *J. Org. Chem.* **83,** 14286–14289 (2018); Hsieh, H. W., Coley, C. W., Baumgartner, L. M., Jensen, K. F. & Robinson, R. I. Photoredox Iridium-Nickel Dual-Catalyzed Decarboxylative Arylation Cross-Coupling: From Batch to Continuous Flow via Self-Optimizing Segmented Flow Reactor. *Org. Process Res. Dev.* **22,** 542–550 (2018); Zhou, Z., Li, X. & Zare, R. N. Optimizing Chemical Reactions with Deep Reinforcement Learning. *ACS Cent. Sci.* **3,** 1337–1344 (2017); Reizman, B. J. & Jensen, K. F. Feedback in Flow for Accelerated Reaction Development. *Acc. Chem. Res.* **49,** 1786–1796 (2016); Fitzpatrick, D. E., Battilocchio, C. & Ley, S. V. A Novel Internet-Based Reaction Monitoring, Control and Autonomous Self-Optimization Platform for Chemical Synthesis. *Org. Process Res. Dev.* **20,** 386–394 (2016); Reizman, B. J., Wang, Y.-M., Buchwald, S. L. & Jensen, K. F. Suzuki–Miyaura cross-coupling optimization enabled by automated feedback. *React. Chem. Eng.* **1,** 658–666 (2016); Cortés-Borda, D. *et al.* Optimizing the Heck–Matsuda Reaction in Flow with a Constraint-Adapted Direct Search Algorithm. *Org. Process Res. Dev.* **20**, 1979-1987 (2016); Reizman, B. J. & Jensen, K. F. Simultaneous solvent screening and reaction optimization in microliter slugs. *Chem. Commun.* **51,** 13290–13293 (2015); McMullen, J. P. & Jensen, K. F. An Automated Microfluidic System for Online Optimization in Chemical Synthesis. *Org. Process Res. Dev.* **14,** 1169–1176 (2010).

[6] Baumgartner, L. M., Coley, C. W., Reizman, B. J., Gao, K. W. & Jensen, K. F. Optimum catalyst selection over continuous and categorical process variables with a single droplet microfluidic reaction platform. *React. Chem. Eng.* **3,** 301–311 (2018); Reizman, B. J., Wang, Y.-M., Buchwald, S. L. & Jensen, K. F. Suzuki-Miyaura–Miyaura cross-coupling optimization enabled by automated feedback. *React. Chem. Eng.* **1,** 658–666 (2016); Reizman, B. J. & Jensen, K. F. Simultaneous solvent screening and reaction optimization in microliter slugs. *Chem. Commun.* **51,** 13290–13293 (2015).

[7] See Reference 5.

[8] Burger, B. *et al.* A mobile robotic chemist. *Nature* **583,** 237–241 (2020); MacLeod, B. P. *et al.* Self-driving laboratory for accelerated discovery of thin-film materials. *Sci. Adv.* **6,** eaaz8867 (2020); Gongora, A. E. *et al.* A Bayesian experimental autonomous researcher for mechanical design. *Sci. Adv.* **6,** eaaz1708 (2020); Langner, S. *et al.* Beyond Ternary OPV: High-Throughput Experimentation and Self-Driving Laboratories Optimize Multicomponent Systems. *Adv. Mater.* **32,** 1907801 (2020).

[9] Häse, F., Roch, L. M., Kreisbeck, C. & Aspuru-Guzik, A. Phoenics: A Bayesian Optimizer for Chemistry. *ACS Cent. Sci.* **4,** 1134–1145 (2018).

[10] Häse, F., Roch, L. M. & Aspuru-Guzik, A. Gryffin: An algorithm for Bayesian optimization for categorical variables informed by physical intuition with applications to chemistry. arXiv:2003.12127 (2020).

[11] Plummer, C. W. *et al.* Design and Synthesis of Novel, Selective GPR40 AgoPAMs. *ACS Med. Chem. Lett.* **8,** 221–226 (2017); Christensen, M. *et al.* Enantioselective synthesis of α-methyl-β-cyclopropyldihydrocinnamates. *J. Org. Chem.* **81,** 824-830 (2016).

[12] For additional palladium-catalyzed stereoselective cross-couplings influenced by phosphine ligands, see: Chehal, N. K., Budzelaar, P. H. M. & Hultin, P. G. E - Z isomerization in Suzuki cross-couplings of haloenones: Ligand effects and evidence for a separate catalytic cycle. *Org. Biomol. Chem.* **16,** 1134–1143 (2018); Lu, G. P., Voigtritter, K. R., Cai, C. & Lipshutz, B. H. Ligand effects on the stereochemistry of Stille couplings, as manifested in reactions of Z-alkenyl halides. *Chem. Commun.* **48,** 8661–8663 (2012); Lu, G. P., Voigtritter, K. R., Cai, C. & Lipshutz, B. H. Ligand effects on the stereochemical outcome of suzuki-miyaura couplings. *J. Org. Chem.* **77,** 3700–3703 (2012); Krasovskiy, A. & Lipshutz, B. H. Ligand effects on Negishi couplings of alkenyl halides. *Org. Lett.* **13,** 3818–3821 (2011).

[13] Johansson Seechurn, C. C. C., Kitching, M. O., Colacot, T. J. & Snieckus, V. Palladium-catalyzed cross-coupling: A historical contextual perspective to the 2010 nobel prize. *Angew. Chem. Int. Ed.* **51,** 5062–5085 (2012). Martin, R. & Buchwald, S. L. Palladium-catalyzed suzuki-miyaura cross-coupling reactions employing dialkylbiaryl phosphine ligands. *Acc. Chem. Res.***41,** 1461–1473 (2008).
[14] Gomes, *et. al.* Mapping the Property Space of Monodentate Organophosphorus Ligands for Catalysis. 10.26434/chemrxiv.12996665 (2020).
[15] Roch, L. M. *et al.* ChemOS: An orchestration software to democratize autonomous discovery. *PLoS One* **15,** e0229862 (2020).
[16] Christensen, M. *et al.* Development of an automated kinetic profiling system with online HPLC for reaction optimization. *React. Chem. Eng.* **4,** 1555–1558 (2019).
[17] Häse, F., Roch, L. M. & Aspuru-Guzik, A. Chimera: Enabling hierarchy based multi-objective optimization for self-driving laboratories. *Chem. Sci.* **9,** 7642–7655 (2018).
[18] Vellanki, P. *et al.* Process-constrained batch Bayesian Optimisation. (2017).
[19] See reference 13.
[20] Zhao, S. *et al.* Enantiodivergent Pd-catalyzed C–C bond formation enabled through ligand parameterization. *Science* **362,** 670–674 (2018); Jover, J. *et al.* Expansion of the Ligand Knowledge Base for Monodentate P-Donor Ligands (LKB-P). *Organometallics* **29,** 6245–6258 (2010); Wu, K. & Doyle, A. G. Parameterization of phosphine ligands demonstrates enhancement of nickel catalysis via remote steric effects. *Nat. Chem.* **9,** 779–784 (2017); Niemeyer, Z. L., Milo, A., Hickey, D. P. & Sigman, M. S. Parameterization of phosphine ligands reveals mechanistic pathways and predicts reaction outcomes. *Nat. Chem.* **8,** 610–617 (2016); Santiago, C. B., Guo, J.-Y. & Sigman, M. S. Predictive and mechanistic multivariate linear regression models for reaction development. *Chem. Sci.* **9,** 2398–2412 (2018); Durand, D. J. & Fey, N. Computational Ligand Descriptors for Catalyst Design. *Chem. Rev.* acs.chemrev.8b00588 (2019).
[21] See Figure 5 for ligand structures.
[22] This cluster contained three low-boiling phosphines, including $P(CF_3)_3$, $PMe(CF_3)_2$ and $PMe_2CF_3$. The same cluster also contained $PMe_2Ac$, a phosphine that was difficult to access commercially or synthetically.
[23] See supplementary information section 6.6 for the selected descriptors and computed properties.
[24] See supplementary information figure SI-9 for the results of campaign 3.
[25] Gensch, *et. al.* Title. 10.26434/chemrxiv.xxxxxxxx (2020).
[26] See supplementary information figure SI-11 for the multivariate linear regression model.
[27] See Reference 14.
[28] See Reference 25.

# SUPPLEMENTARY INFORMATION

## Data-science driven autonomous process optimization

Melodie Christensen[1,2], Lars P.E. Yunker[1], Folarin Adedeji[2], Florian Häse[3,4,5,7,9], Loïc M. Roch[3,4,5,9], Tobias Gensch[6], Gabriel dos Passos Gomes[4,5,7], Tara Zepel[1], Matthew S. Sigman*[6], Alán Aspuru-Guzik*[3,4,5,7,8] and Jason E. Hein[1*]

[1]*Department of Chemistry, University of British Columbia, Vancouver, British Columbia V6T 1Z1, Canada.*
[2]*Department of Process Research and Development, Merck & Co., Inc., Rahway, NJ 07065, United States.*
[3]*Department of Chemistry and Chemical Biology, Harvard University, Cambridge, MA 02138, United States.*
[4]*Department of Chemistry, University of Toronto, Toronto, Ontario M5S 3H6, Canada.*
[5]*Department of Computer Science, University of Toronto, Toronto, Ontario M5T 3A1, Canada.*
[6]*Department of Chemistry, University of Utah, Salt Lake City, Utah 84112, United States.*
[7]*Vector Institute for Artificial Intelligence, Toronto, Ontario M5S 1M1, Canada.*
[8]*Canadian Institute for Advanced Research, Toronto, Ontario M5G 1Z8, Canada.*
[9]*ChemOS Sàrl, Lausanne, Vaud 1006, Switzerland.*

**Corresponding authors: Matthew S. Sigman sigman@chem.utah.edu, Alán Aspuru-Guzik aspuru@utoronto.ca, Jason E. Hein jhein@chem.ubc.ca*

# Table of Contents


**1. General remarks** ..... 3

1.1 Chemical suppliers ..... 3

1.2 Equipment ..... 3

1.3 Analytical methods ..... 4

**2. Experimental procedures** ..... 5

2.1 Procedure for stock mixture preparations ..... 5

2.2 Procedure for autonomous optimization experiments ..... 9

2.3 Procedure for manual experiments ..... 10

2.4 Procedures for the preparation of non-commercial compounds ..... 11

**4. Autonomous optimization protocol** ..... 14

4.1 Sample csv file with dispense volumes ..... 14

4.2 Sample Chemspeed Autosuite protocol ..... 14

**5. Machine learning algorithms** ..... 16

5.1 Process constrained optimization in the context of autonomous experimentation ..... 16

**6. Analytical data** ..... 17

6.1 $^{1}$H NMR weight % purity determinations ..... 17

6.2 Calibration curves ..... 19

6.3 Preliminary data ..... 20

6.4 Campaign 1 data ..... 21

6.5 Campaign 2 data ..... 24

6.6 Campaign 3 data ..... 28

6.7 Campaign 3 visualization ..... 33

6.8 Standard experiments ..... 34

**7. Predictive model** ..... 35

## 1. General remarks

### 1.1 Chemical suppliers

Commercial reagents were purchased from Millipore Sigma, Oakwood, Combi-Blocks, Alfa Aesar, Acros, Strem, Apollo and Alichem and used as received. Anhydrous solvents were purchased from Millipore Sigma and used as received. Aqueous solutions were deoxygenated through subsurface nitrogen sparge for a minimum of 30 minutes.

### 1.2 Equipment

Flash chromatography was performed on a CombiFlash purification system employing Redisep Rf Gold silica gel columns. $^{1}H$ NMR spectra for weight % purity determinations were recorded on a Bruker 500 MHz instrument with a delay time of 20 sec and 32 scans. Samples were prepared in $CDCl_3$ and spectra were calibrated to the $CDCl_3$ reference peak at 7.26 ppm.

Autonomous optimization experiments were carried out on a Chemspeed Swing liquid handling robot equipped with an adjustable-pitch four needle (0.8 mm ID) liquid dispense tool, a V&P Scientific tumble stirrer and a Huber Unistat 82T chiller. The robot was integrated with an Agilent 1100 HPLC-UV system through installation of a two position, 6-port HPLC valve on the Chemspeed Swing deck and connection to the Agilent 1100 through 0.17 mm ID tubing. Valve switching and chromatographic resolutions were triggered through contact closures.

Reactions were carried out in 96-well aluminum reaction blocks (Analytical Sales 96973) with 8 x 30 mm glass vial inserts (Analytical Sales 884001). Vials were sealed with a layer of two PFA films (Analytical Sales 96967), one tan fluoropolymer mat (Analytical Sales 78040) and a custom aluminum needle-guiding top cover (figure SI-1). Vigorous agitation was achieved with 5 mm PVDF-encapsulated NdFeB magnetic tumble stir discs (VP 772DP-N42-5-2). Reaction aliquots were sampled into 96-well dilution plates (Analytical Sales 17P687) capped with pre-slit silicone/PTFE cap mats (Analytical Sales 965075).

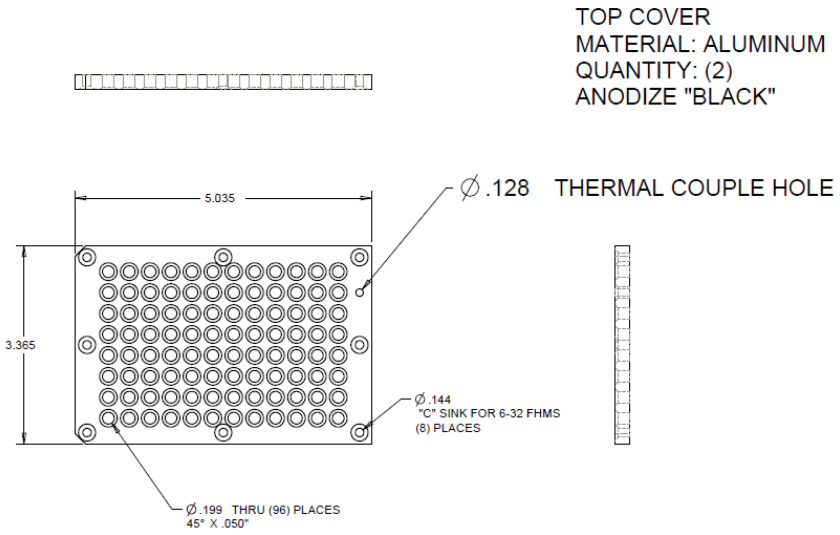


**Figure SI-1. Custom aluminum needle-guiding top cover**

1.3 Analytical methods

Reaction analysis was carried out through utilization of the HPLC-UV method described in Table SI-1.

**Table SI-1. HPLC-UV method for yield determination**

| | | |
|---|---|---|
| Column: | Cortecs C18 2.7 um, 4.6 x 150 mm | |
| Column Temperature: | 55 °C | |
| Flow Rate: | 1.5 ml/min | |
| Detection: | 210 nm | |
| Acquisition Time: | 10 min | |
| Mobile Phase: | Solvent A = 2 mM ammonium formate in water;<br>Solvent B = 2 mM ammonium formate in acetonitrile 10% water | |
| Mobile Phase Program: | Time<br>0.00 min<br>6.00 min<br>8.00 min<br>8.10 min<br>10.00 min | B%<br>5<br>95<br>95<br>5<br>5 |
| Injection Volume: | 5 µL | |
| Compound Name: | Retention time: | |
| 3-(benzyloxy)phenyl)boronic acid | 4.75 min | |
| 1,3,5-trimethoxybenzene | 4.93 min | |
| (*E*)-Methyl 3-cyclopropyl-2-methyl-3-(tosyloxy)acrylate (**1-*E***) | 6.13 min | |
| (*Z*)-Methyl 3-(3-(benzyloxy)phenyl)-3-cyclopropyl-2-methylacrylate (**2-*Z***) | 6.98 min | |
| (*E*)-Methyl 3-(3-(benzyloxy)phenyl)-3-cyclopropyl-2-methylacrylate (**2-*E***) | 7.10 min | |
| Example Chromatogram | | |

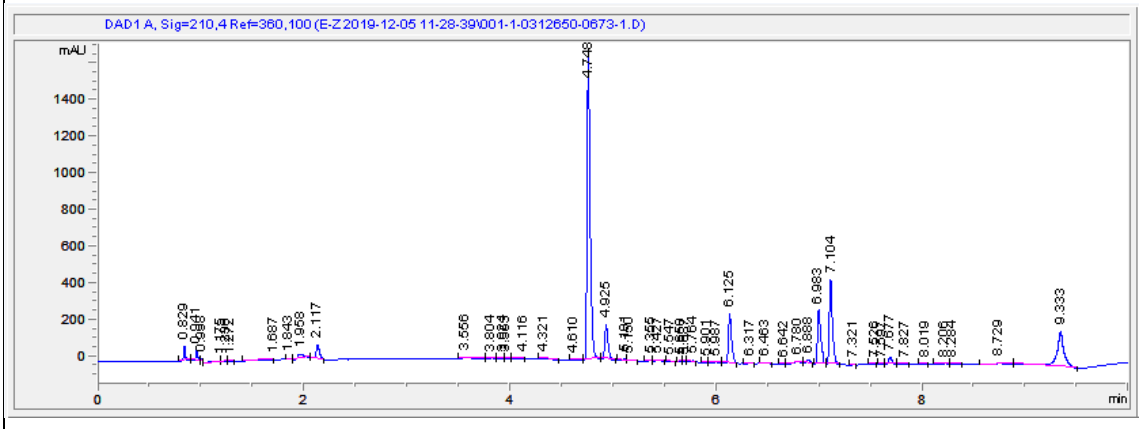

## 2. Experimental procedures

### 2.1 Procedure for stock mixture preparations

Fresh stock mixtures were prepared in 4 - 20 ml vials in a positive nitrogen pressure glove box, sealed with septa caps and transferred to the positive nitrogen pressure Chemspeed robot deck. Stock mixture concentrations were selected based on factors such as solubility, minimum accurate dispense volume, and a 200 µl total organic reaction volume (Tables SI-2 and SI-3). The mixtures were prepared by weighing the solids or oils on an analytical balance followed by adding anhydrous ACN through manual pipetting. The recipes followed in stock mixture preparation are provided in Tables SI-4 and SI-5.

**Table SI-2. Campaign 1 stock mixture concentrations and parameter ranges**

| Chemical | Eq low | Eq high | µmol low | µmol high | µl low | µl high | M |
|---|---|---|---|---|---|---|---|
| $Pd(ACN)_2Cl_2$ | 0.01 | 0.05 | 0.1 | 0.5 | 10 | 50 | 0.010 |
| P Ligand | 0.005 | 0.20 | 0.05 | 2 | 1 | 50 | 0.040 |
| E-Tosyl | 1.00 | 1.00 | 10 | 10 | 20 | 20 | 0.500 |
| IS | 0.10 | 0.10 | 1 | 1 | | | 0.050 |
| ArBA | 1.00 | 2.00 | 10 | 20 | 40 | 80 | 0.250 |
| $K_3PO_4$ | 3.00 | 3.00 | 30 | 30 | 60 | 60 | 0.500 |
| ACN | | | | | 129 | | |
| Total Org | | | | | 200 | 200 | |
| Total Aq | | | | | 60 | 60 | |

**Table SI-3. Campaigns 2 and 3 stock mixture concentrations and parameter ranges**

| Chem | Eq low | Eq high | µmol low | µmol high | µl low | µl high | M |
|---|---|---|---|---|---|---|---|
| $Pd(ACN)_2Cl_2$ | 0.01 | 0.05 | 0.1 | 0.5 | 10 | 50 | 0.010 |
| P Ligand | 0.01 | 0.20 | 0.05 | 2 | 3 | 100 | 0.020 |
| E-Tosyl | 1.00 | 1.00 | 10 | 10 | 20 | 20 | 0.500 |
| IS | 0.10 | 0.10 | 1 | 1 | | | 0.050 |
| ArBA | 1.50 | 1.50 | 15 | 15 | 30 | 30 | 0.500 |
| $K_3PO_4$ | 3.00 | 3.00 | 30 | 30 | 60 | 60 | 0.500 |
| ACN | | | | | 138 | | |
| Total Org | | | | | 200 | 200 | |

| | | | |
|---|---|---|---|
| Total Aq | | 60 | 60 |

**Table SI-4. Campaign 1 stock mixture recipes**

| Mixture | Chemical | MW (g/mol) | Amount (mg) | Density (g/ml)* | Amount (ml) |
|---|---|---|---|---|---|
| $Pd(ACN)_2Cl_2$ | 14592-56-4 | 259.43 | 31.13 | 1.00 | 0.03 |
| | ACN | 41.05 | | 0.79 | 11.97 |
| $PPh_3$ (**L1**) | 603-35-0 | 262.29 | 125.90 | 1.00 | 0.13 |
| | ACN | 41.05 | | 0.79 | 11.87 |
| $PoTol_3$ (**L2**) | 6163-58-2 | 304.37 | 146.10 | 1.00 | 0.15 |
| | ACN | 41.05 | | 0.79 | 11.85 |
| $PtBu_3.HBF_4$ (**L3**) | 131274-22-1 | 202.32 | 97.11 | 1.00 | 0.10 |
| | ACN | 41.05 | | 0.79 | 11.90 |
| AtaPhos (**L4**) | 932710-63-9 | 265.38 | 127.38 | 1.00 | 0.13 |
| | ACN | 41.05 | | 0.79 | 11.87 |
| MorDalPhos (**L5**) | 1237588-12-3 | 463.65 | 222.55 | 1.00 | 0.22 |
| | ACN | 41.05 | | 0.79 | 11.78 |
| QPhos (**L6**) | 312959-24-3 | 710.72 | 341.15 | 1.00 | 0.34 |
| | ACN | 41.05 | | 0.79 | 11.66 |
| DPPF (**L7**) | 12150-46-8 | 554.39 | 266.11 | 1.00 | 0.27 |
| | ACN | 41.05 | | 0.79 | 11.73 |
| DTBPF (**L8**) | 84680-95-5 | 474.43 | 227.73 | 1.00 | 0.23 |
| | ACN | 41.05 | | 0.79 | 11.77 |
| XPhos (**L9**) | 564483-18-7 | 476.73 | 228.83 | 1.00 | 0.23 |
| | ACN | 41.05 | | 0.79 | 11.77 |
| BrettPhos (**L10**) | 1070663-78-3 | 536.78 | 257.65 | 1.00 | 0.26 |
| | ACN | 41.05 | | 0.79 | 11.74 |
| AdBrettPhos (**L11**) | 1160861-59-5 | 640.93 | 307.65 | 1.00 | 0.31 |
| | ACN | 41.05 | | 0.79 | 11.69 |

| | | | | | |
|---|---|---|---|---|---|
| RockPhos (**L12**) | 1262046-34-3 | 468.71 | 224.98 | 1.00 | 0.22 |
| | ACN | 41.05 | | 0.79 | 11.78 |
| E-Tos | E-Tos (**1-*E***) | 310.36 | 744.87 | 1.00 | 0.74 |
| | 1,3,5-trimethoxybenzene | 168.19 | 40.37 | 1.00 | 0.04 |
| | ACN | 41.05 | | 0.79 | 4.01 |
| ArBA | ArBA (**3**) | 228.05 | 1094.64 | 1.00 | 1.09 |
| | Water | 18.02 | | 1.00 | 0.91 |
| | ACN | 41.05 | | 0.79 | 18.11 |
| $K_3PO_4$ | potassium phosphate, tribasic | 212.27 | 3056.62 | 1.00 | 3.06 |
| | ACN | 41.05 | | 0.79 | 25.74 |

*Density of 1.00 g/ml was assumed for all solids.

**Table SI-5. Campaigns 2 and 3 stock mixture recipes**

| **Mixture** | **Chemical** | **MW** | **Amount (mg)** | **Density (g/ml)*** | **Amount (ml)** |
|---|---|---|---|---|---|
| $Pd(ACN)_2Cl_2$ | 14592-56-4 | 259.43 | 37.36 | 1.00 | 0.04 |
| | ACN | 41.05 | | 0.79 | 14.36 |
| $PEt_3$ (**L13**) | 554-70-1 | 118.16 | 17.02 | 0.80 | 0.0212 |
| | ACN | 41.05 | | 0.79 | 7.18 |
| $PCy_2Ph$ (**L19**) | 6476-37-5 | 274.38 | 39.51 | 1.00 | 0.04 |
| | ACN | 41.05 | | 0.79 | 7.16 |
| 1-$Cy_2$P-2',4',6'-MeO-$Ph_2$ (**L28**) | 1000171-05-0 | 440.55 | 63.44 | 1.00 | 0.06 |
| | ACN | 41.05 | | 0.79 | 7.14 |
| $PPh_2$(2,6-Me-Ph) (**L20**) | 117672-33-0 | 290.34 | 41.81 | 1.00 | 0.04 |
| | ACN | 41.05 | | 0.79 | 7.16 |
| $PPh_2$(2-OMe-Ph) (**L21**) | 53111-20-9 | 292.31 | 42.09 | 1.00 | 0.04 |
| | ACN | 41.05 | | 0.79 | 7.16 |
| Pallyl$Ph_2$ (**L22**) | 2741-38-0 | 226.25 | 32.58 | 1.05 | 0.03 |
| | ACN | 41.05 | | 0.79 | 7.17 |
| JohnPhos (**L29**) | 224311-51-7 | 298.40 | 42.97 | 1.00 | 0.04 |

| | | | | | |
|---|---|---|---|---|---|
| | ACN | 41.05 | | 0.79 | 7.16 |
| $P(C_6F_5)_2Ph$ (**L23**) | 5074-71-5 | 442.20 | 63.68 | 1.00 | 0.06 |
| | ACN | 41.05 | | 0.79 | 7.14 |
| RockPhos (**L12**) | 1262046-34-3 | 468.69 | 67.49 | 1.00 | 0.07 |
| | ACN | 41.05 | | 0.79 | 7.13 |
| PhAtaPhos (**L24**) | 739-58-2 | 305.35 | 43.97 | 1.00 | 0.04 |
| | ACN | 41.05 | | 0.79 | 7.16 |
| SPhos (**L31**) | 657408-07-6 | 410.53 | 59.12 | 1.00 | 0.06 |
| | ACN | 41.05 | | 0.79 | 7.14 |
| (R)SITCP (**L18**) | 856407-37-9 | 354.42 | 51.04 | 1.00 | 0.05 |
| | ACN | 41.05 | | 0.79 | 7.15 |
| $P(mesityl)_3$ (**L14**) | 23897-15-6 | 388.52 | 55.95 | 1.00 | 0.06 |
| | ACN | 41.05 | | 0.79 | 7.14 |
| P(3,5-Me-4-OMe-$Ph)_3$ (**L15**) | 121898-64-4 | 436.52 | 62.86 | 1.00 | 0.06 |
| | ACN | 41.05 | | 0.79 | 7.14 |
| Et-PhenCarPhos (**L32**) | 1308652-66-5 | 331.39 | 47.72 | 1.00 | 0.05 |
| | ACN | 41.05 | | 0.79 | 7.15 |
| $PoTol_3$ (**L2**) | 6163-58-2 | 304.37 | 43.83 | 1.00 | 0.04 |
| | ACN | 41.05 | | 0.79 | 7.16 |
| $Ph_2P(CH_2)_3Si(OEt)_3$ (**L25**) | 52090-23-0 | 390.53 | 56.24 | 1.00 | 0.06 |
| | ACN | 41.05 | | 0.79 | 7.14 |
| PPh(4-(2,2-$CF_3$-$F_7$pent)-$Ph)_2$ (**L26**) | 322647-83-6 | 926.41 | 133.40 | 1.00 | 0.13 |
| | ACN | 41.05 | | 0.79 | 7.07 |
| m-CroPhos (**L27**) | 1620882-90-7 | 200.30 | 28.84 | 1.00 | 0.03 |
| | ACN | 41.05 | | 0.79 | 7.17 |
| AtaPhos (**L4**) | 932710-63-9 | 265.37 | 38.21 | 1.00 | 0.04 |
| | ACN | 41.05 | | 0.79 | 7.16 |
| PhSPhos (**L30**) | 819867-24-8 | 398.43 | 57.37 | 1.00 | 0.06 |

| | | | | | |
|---|---|---|---|---|---|
| | ACN | 41.05 | | 0.79 | 7.14 |
| $P(nOct)_3$ (**L16**) | 4731-53-7 | 370.64 | 53.37 | 0.83 | 0.06 |
| | ACN | 41.05 | | 0.79 | 7.14 |
| $PnPr_3$ (**L17**) | 2234-97-1 | 160.24 | 23.07 | 0.80 | 0.0288 |
| | ACN | 41.05 | | 0.79 | |
| E-Tos | E-Tos (**1-*E***) | 310.36 | 893.85 | 1.00 | 0.89 |
| | 1,3,5-trimethoxybenzene | 168.19 | 48.44 | 1.00 | 0.05 |
| | ACN | 41.05 | | 0.79 | 4.82 |
| ArBA | ArBA (**3**) | 228.05 | 985.18 | 1.00 | 0.99 |
| | Water | 18.02 | | 1.00 | 0.38 |
| | ACN | 41.05 | | 0.79 | 7.65 |
| $K_3PO_4$ | potassium phosphate, tribasic | 212.27 | 2445.29 | 1.00 | 2.45 |
| | ACN | 41.05 | | 0.79 | 20.59 |

*Density of 1.00 g/ml was assumed for all solids.

2.2 Procedure for autonomous optimization experiments

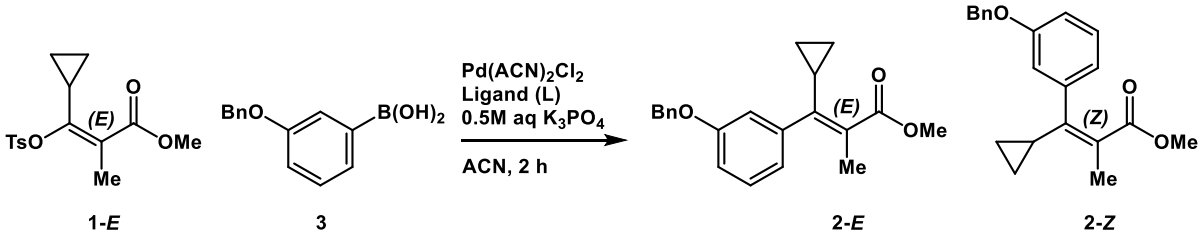


1-*E* 3 2-*E* 2-*Z*

*General:* Two fluoropolymer and PFA mat-sealed 96-well metal blocks with 1 mL glass vial inserts were equilibrated at the designated reaction temperature under 20 psig of nitrogen with 500 rpm agitation.

*Representative procedure for test reactions:* In campaigns involving 192 iterations, eight wells from each 96-well reaction block were dedicated to standard reactions to test for reproducibility. To each well was dispensed $Pd(ACN)_2Cl_2$ (0.25 µmol, 25 µl of 0.01 M stock solution), and **L2** ($PoTol_3$) (0.38 µmol, 19 µl of 0.02 M stock mixture), followed by 7 min of age time. Then, *E*-tosylate **1-*E*** (10 µmol) with 1,3,5-trimethoxybenzene (1 µmol) was dispensed (20 µl of 0.5 M/ 0.05 M stock solution), followed by (3-(benzyloxy)phenyl)boronic acid **3** (15 µmol, 30 µl of 0.5 M stock solution in degassed ACN 5% $H_2O$), followed by anhydrous ACN (106 µl) to ensure a total organic solvent volume of 200 µl. Then, a dispense of degassed aqueous $K_3PO_4$ (30 µmol, 60 µl of 0.5 M stock solution) was carried out to initiate the reaction. This procedure was executed sequentially for each well within a loop of eight replicates in 15-minute intervals. Each replicate was time stamped individually, aged for 120 min, and sampled for online analysis.

*Representative procedure for optimization reactions:* In campaigns involving 192 iterations, 88 wells from each 96-well reaction block were dedicated to the optimization reactions. To each well was dispensed $Pd(ACN)_2Cl_2$ (0.1 - 0.5 µmol, 10 - 50 µl of 0.01 M stock solution), and phosphine ligand (0.05 - 2.0 µmol, 3

- 100 µl of 0.02 M stock mixture), followed by 7 min of age time. Then, E-tosylate **1-*E*** (10 µmol) with 1,3,5-trimethoxybenzene (1.0 µmol) was dispensed (20 µl of 0.5 M/ 0.05 M stock solution), followed by (3-(benzyloxy)phenyl)boronic acid **3** (15 µmol, 30 µl of 0.5 M stock solution in degassed ACN 5% $H_2O$), followed by anhydrous ACN (0 - 138 µl) to ensure a total organic solvent volume of 200 µl. Then, a dispense of degassed aqueous $K_3PO_4$ (30 µmol, 60 µl of 0.5 M stock solution) was carried out to initiate the reaction. This procedure was executed sequentially for each well within a loop of eight experiments in 15-minute intervals. Each reaction was time stamped individually, aged for 120 min, and sampled for online analysis.

*Sampling and analysis:* Two polypropylene 96-well collection blocks sealed with a silicone mats were manually prefilled with 800 µl of acetonitrile 10% aqueous pH 3.5 ammonium formate buffer and placed on the robot deck. Upon reaching the reaction end point at 120 min, 10 ul of reaction mixture was aliquoted and dispensed into the 800 ul quench solution in the collection block. Upon needle-mixing, 40 ul of quenched sample from the collection block was aliquoted and injected to the on-deck sampling valve outfitted with a 5 µl loop. The valve was automatically switched to transfer the sample to the Agilent 1100 HPLC for analysis.

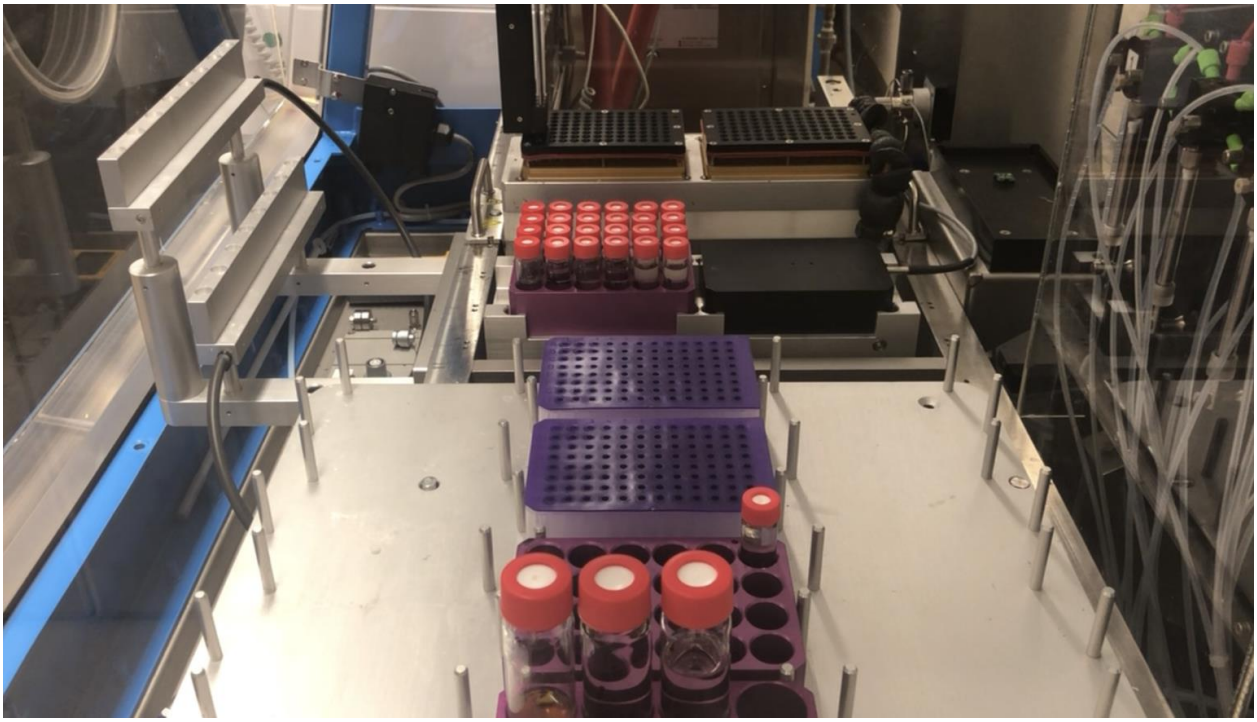

**Figure SI-2: Chemspeed robot deck during autonomous experiments**

2.3 Procedure for manual experiments

Manual experiments were carried out in in a positive nitrogen pressure glove box, in 96-well aluminum reaction blocks with 8 x 30 mm glass vial inserts. To each well was pipet dispensed $Pd(ACN)_2Cl_2$ (0.38 µmol, 38 µl of 0.01 M stock solution), and phosphine ligand (0.92 µmol, 46 µl of 0.02 M stock mixture), followed by 7 min of age time. Then, *E*-tosylate **1-*E*** (10 µmol) with 1,3,5-trimethoxybenzene (1 µmol) was pipet dispensed (20 µl of 0.5 M/ 0.05 M stock solution), followed by (3-(benzyloxy)phenyl)boronic acid **3** (15 µmol, 30 µl of 0.5 M stock solution in degassed ACN 5% $H_2O$), followed by anhydrous ACN (66 µl) to ensure a total organic solvent volume of 200 µl. Then, degassed aqueous $K_3PO_4$ (30 µmol, 60 µl of 0.5 M stock

solution) was pipet dispensed. The block was sealed and agitated for 120 minutes at 35 °C under 400 rpm tumble stirring. Upon reaction completion, 10 ul of reaction mixture was aliquoted and quenched into 800 µl of acetonitrile 10% aqueous pH 3.5 ammonium formate buffer. Each sample was analyzed via the Chemspeed online HPLC for consistency.

2.4 Procedures for the preparation of non-commercial compounds

*Methyl 3-cyclopropyl-2-methyl-3-oxopropanoate **5**:*

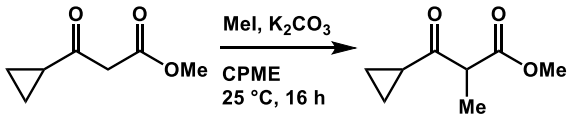


4 5

To a round-bottomed flask under nitrogen atmosphere was charged methyl 3-cyclopropyl-3-oxopropanoate **4** (40.0 g, 281 mmol), methyl iodide (17.6 ml, 281 mmol), $K_2CO_3$ (58.3 g, 422 mmol) and CPME (100 ml). The reaction was agitated at 25° C for 1.5 h. Additional methyl iodide (17.6 ml, 281 mmol) was charged and the reaction was agitated at 25° C for an additional 16 h. $K_2CO_3$ was removed through filtration and the cake was washed with CPME (50 ml). The filtrate was concentrated to an oil that was purified by normal phase column chromatography to give methyl 3-cyclopropyl-2-methyl-3-oxopropanoate **5**[1] in 59% yield.

*(E)-Methyl 3-cyclopropyl-2-methyl-3-(tosyloxy)acrylate **1-E**:*

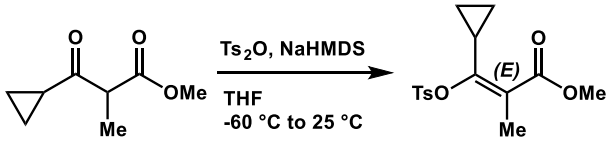


5 1-*E*

To an oven-dried round-bottomed flask under nitrogen atmosphere was added methyl 3-cyclopropyl-2-methyl-3-oxopropanoate **5** (26.0 g, 166 mmol) and THF (260 ml). The mixture was cooled to -78 °C and 1M NaHMDS solution (200 ml, 200 mmol) was added over 20 min, maintaining the internal temperature below -60 °C, followed by a THF rinse (65 ml). The reaction was agitated at -78 °C for 20 min and $Ts_2O$ (65.2 g, 200 mmol) in THF (520 ml) was added over 20 min, maintaining the internal temperature below -60 °C. The reaction was agitated at -78 °C for 20 min, then warmed to 25 °C and agitated for 16 h. A thick slurry formed. The reaction was quenched with 750 ml of aqueous 0.5M $NaHCO_3$ and the phases were separated. The aqueous layer was back-extracted twice with 250 ml of EtOAc. The organic layers were combined and washed with 500 ml of saturated aqueous NaCl, dried over $MgSO_4$ and filtered. Upon concentration to an oil, the crude product was purified by normal phase column chromatography to give (*E*)-methyl 3-cyclopropyl-2-methyl-3-(tosyloxy)acrylate **1-*E***[1] in 31% yield.

*(E)-Methyl 3-(3-(benzyloxy)phenyl)-3-cyclopropyl-2-methylacrylate **2-E** and (Z)-Methyl 3-(3-(benzyloxy)phenyl)-3-cyclopropyl-2-methylacrylate **2-Z**:*

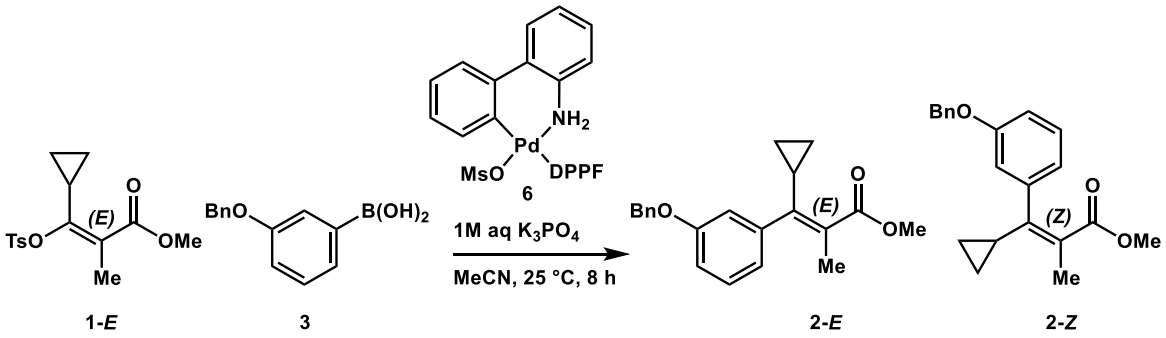


To a reaction vial in a positive nitrogen pressure glove box was charged (*E*)-methyl 3-cyclopropyl-2-methyl-3-(tosyloxy)acrylate **1-*E*** (1.00 g, 3.22 mmol), (3-(benzyloxy)phenyl)boronic acid **3** (0.808 g, 3.54 mmol), and palladium precatalyst **6** (0.298 g, 0.322 mmol). Anhydrous ACN (15 ml) and degassed 1M aqueous $K_3PO_4$ (9.67 ml, 9.67 mmol) were added and the reaction was agitated at 25 °C for 8 h. To the reaction was added 10 ml of saturated aqueous $NH_4Cl$ and the organic layer was separated from the aqueous layer. The aqueous layer was back-extracted twice with 10 ml of EtOAc. The combined organic layers were washed with 10 ml of saturated aqueous NaCl, dried over $MgSO_4$ and filtered. Upon concentration to an oil, the crude product was purified by normal phase column chromatography to give (*E*)-methyl 3-(3-(benzyloxy)phenyl)-3-cyclopropyl-2-methylacrylate **2-*E***[2] in 52% and (*Z*)-methyl 3-(3-(benzyloxy)phenyl)-3-cyclopropyl-2-methylacrylate **2-*Z***[1] in 33% yield.

*(2,6-dimethylphenyl)diphenylphosphane **L20**:*

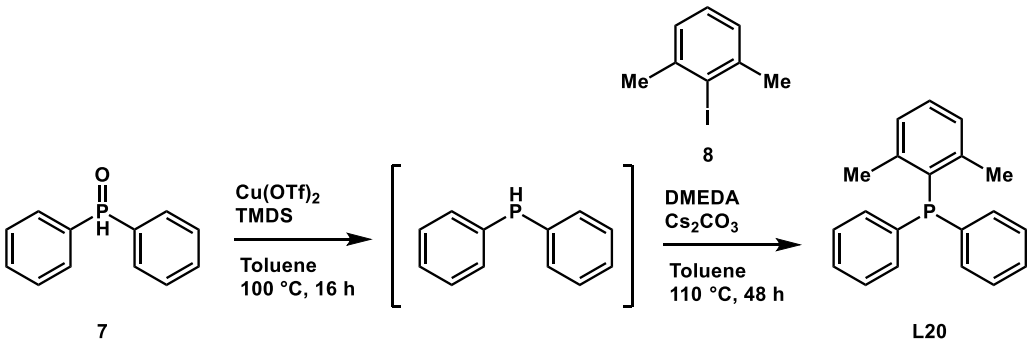


To a reaction vial in a positive nitrogen pressure glove box was charged $Cu(OTf)_2$ (0.268 g, 0.742 mmol), diphenylphosphine oxide **7** (1.00 g, 4.95 mmol), anhydrous toluene (20 ml) and TMDS (1.76 ml, 9.89 mmol). The reaction was agitated at 100 °C for 5 h with needle venting to avoid pressure build-up. Additional TMDS (0.868 ml, 4.95 mmol) was charged and the reaction was agitated at 100 °C for an additional 16 h with no venting. Upon cooling to 25 °C, to the reaction vial was added DMEDA (0.106 ml, 0.989 mmol), $Cs_2CO_3$ (3.22 g, 9.89 mmol) and 2-iodo-1,3-dimethylbenzene **8** (1.15 g, 4.95 mmol). The suspension was agitated at 110 °C for 48 h. The reaction was cooled to 0 °C and KOH (20.6 ml, 61.8 mmol) in MeOH (3N) was added slowly to maintain the temperature below 0 °C. The mixture was agitated at 25 °C for 5 h. The quenched mixture was removed from the glovebox and 30 ml water was added. The resulting solution was back-extracted three times with 50 ml EtOAc. The combined organic layers were washed with 50 ml of 1M aqueous HCl, followed by 50 ml of 0.5M aqueous $NaHCO_3$. The organic layer was decanted to remove elemental copper, dried over $Na_2SO_4$ and filtered. Upon concentration to an oil,

the crude product was purified by normal phase column chromatography to give (2,6-dimethylphenyl)diphenylphosphane **L20**[3] in 13% yield.

### 3. Data integration script

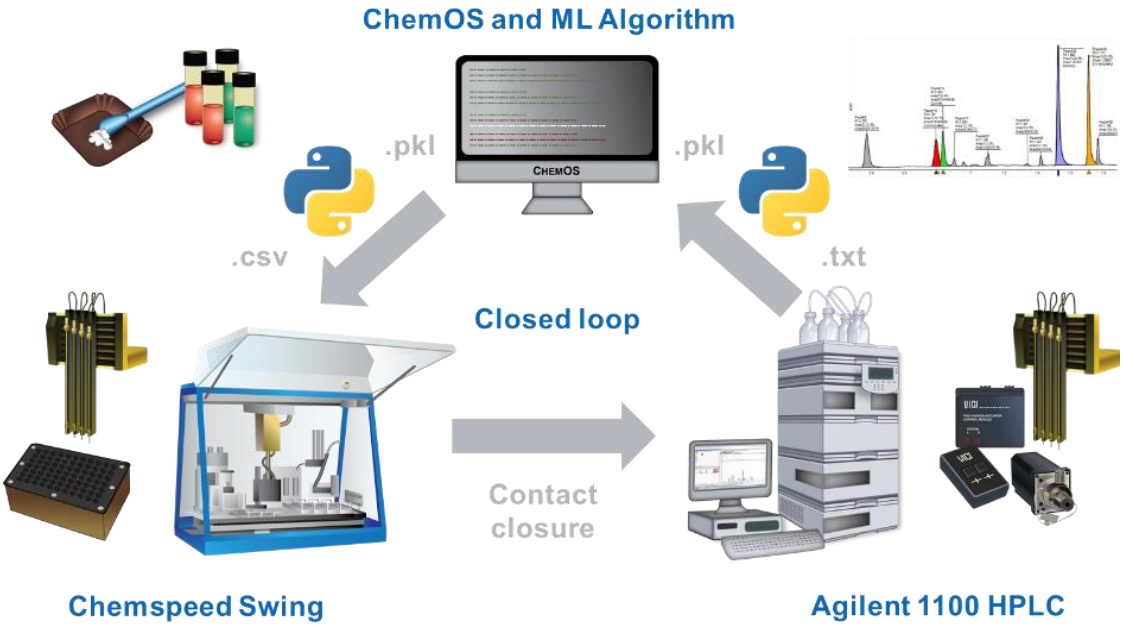


**Figure SI-3: Schematic of data integration established through Python**

The Python script used in this work provided an interface between the tools involved in the optimization. This script performed three primary operations: receiving instructions from ChemOS, conveying them to the Chemspeed, monitoring for HPLC results, and conveying those results back to ChemOS. The script has been made publicly available on Gitlab under the MIT open source license.

ChemOS parameters were conveyed to the experimental computer via a file syncing service in the form of pickled dictionaries (dictionaries written to file with Python's pickle standard library). Parameter values were provided in ratios and equivalents, which were converted to volumes for the Chemspeed to dispense based on stored concentrations. Stock mixture concentrations were defined in a separate file, and all dispensing volumes were determined by their relation to the volume and concentration of the vinyl tosylate (held constant for every reaction). For every value, the volume to dispense was determined, rounded to the nearest microliter (the smallest practically accurate volume that the Chemspeed SWING was capable of dispensing), then back-calculated to the actual ratio used. The parameter dictionary was updated with these values so that ChemOS was provided with the true values used to run the experiment. Finally, the total volume was calculated and the total well volume was made up to 200 µL with acetonitrile. Every volume was then written to a csv file which the Chemspeed was programmed to reference for dispensing volumes.

For interpreting and returning experiment result to Chemspeed, the script monitored the sample data directory for the Agilent HPLC. The HPLC method was configured to output a text report after method

completion, which the script parsed and related to the E- and Z-product peaks by retention time, and a predetermined response factor was used to calculate the assay yield. The result data was then returned to ChemOS via the file syncing service.

## 4. Autonomous optimization protocol

### 4.1 Sample csv file with dispense volumes

The sample csv file below was generated through the Python script as ChemOS instructions became available. This file was automatically referenced in the Chemspeed Autosuite protocol for dispense volumes with each column being mapped to a distinct protocol source zone. The Python script also recorded analytical results to this csv file as Chemstation report files became available, mainly for recordkeeping purposes.

2019-12-04
chemspeed values.c

### 4.2 Sample Chemspeed Autosuite protocol

The below Chemspeed Autosuite protocol was executed in campaigns 2 and 3, running autonomously over four days.

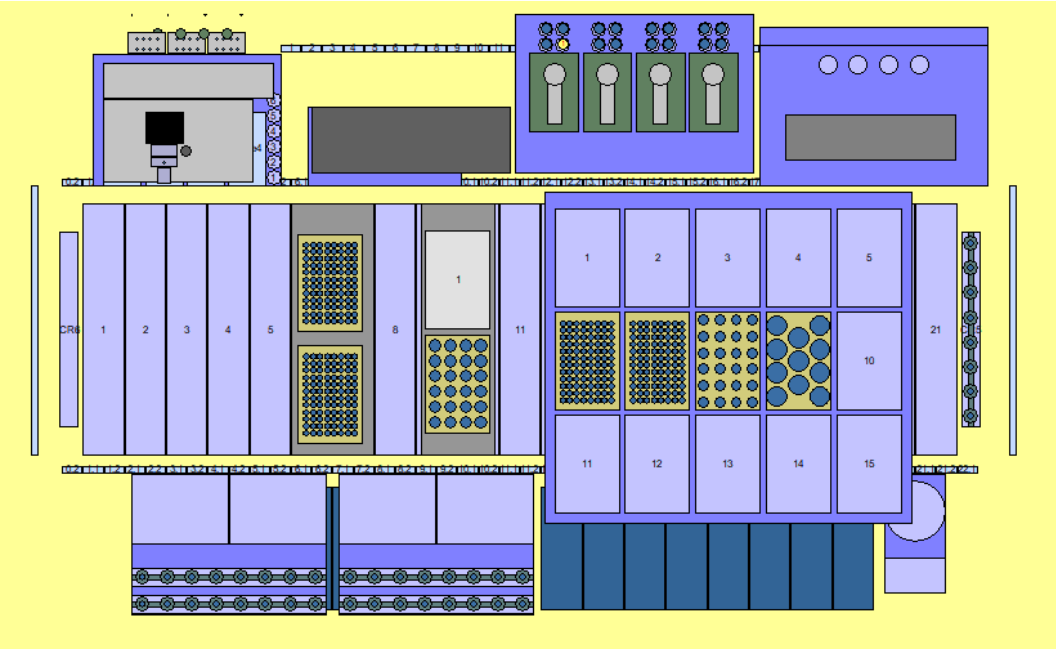

**Figure SI-4: Chemspeed deck layout**

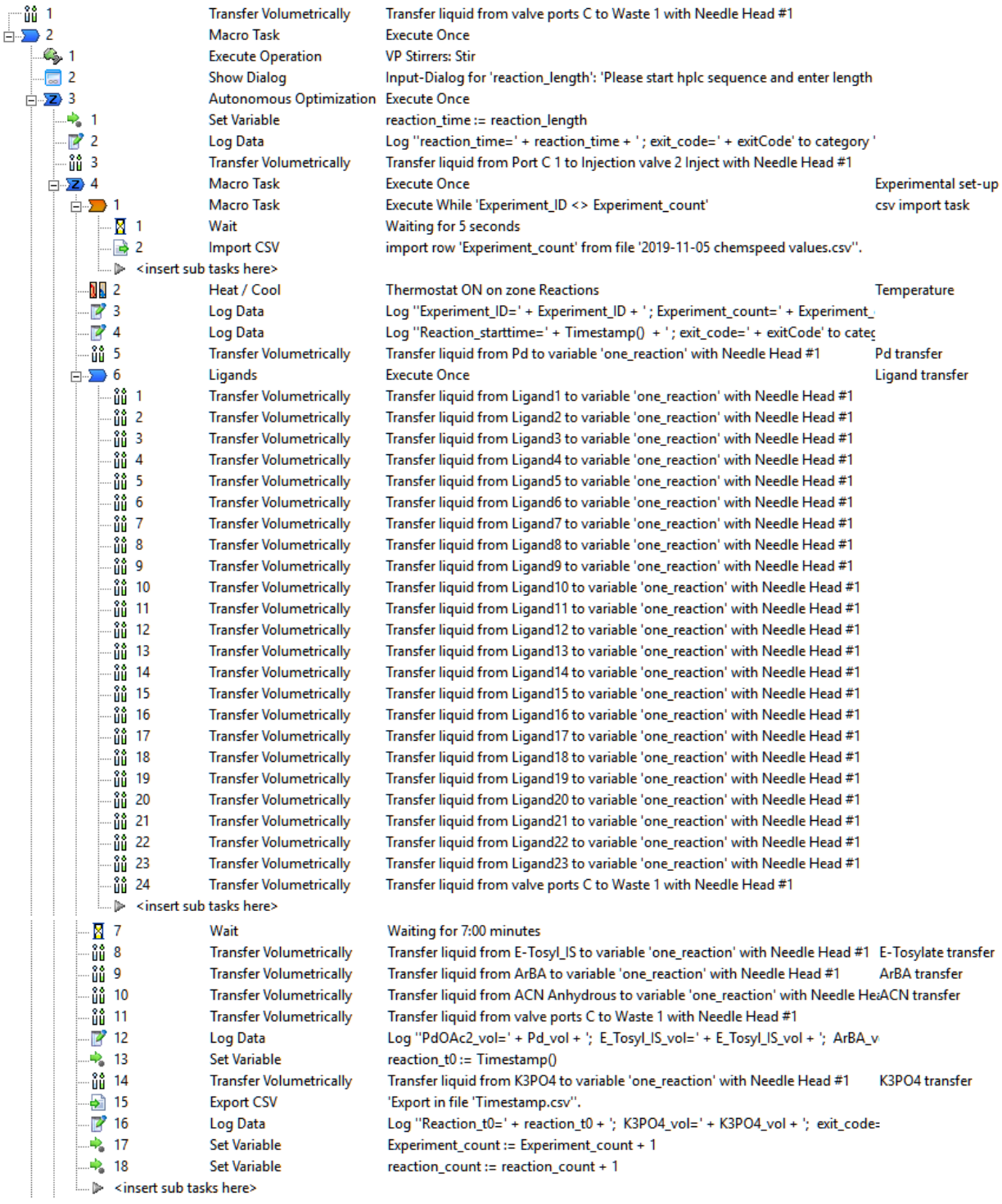
1 Transfer Volumetrically Transfer liquid from valve ports C to Waste 1 with Needle Head #1
2 Macro Task Execute Once
1 Execute Operation VP Stirrers: Stir
2 Show Dialog Input-Dialog for 'reaction_length': 'Please start hplc sequence and enter length
3 Autonomous Optimization Execute Once
1 Set Variable reaction_time := reaction_length
2 Log Data Log ''reaction_time=' + reaction_time + ' ; exit_code=' + exitCode' to category '
3 Transfer Volumetrically Transfer liquid from Port C 1 to Injection valve 2 Inject with Needle Head #1
4 Macro Task Execute Once Experimental set-up
1 Macro Task Execute While 'Experiment_ID <> Experiment_count' csv import task
1 Wait Waiting for 5 seconds
2 Import CSV import row 'Experiment_count' from file '2019-11-05 chemspeed values.csv''.
<insert sub tasks here>
2 Heat / Cool Thermostat ON on zone Reactions Temperature
3 Log Data Log ''Experiment_ID=' + Experiment_ID + ' ; Experiment_count=' + Experiment_
4 Log Data Log ''Reaction_starttime=' + Timestamp() + ' ; exit_code=' + exitCode' to cate
5 Transfer Volumetrically Transfer liquid from Pd to variable 'one_reaction' with Needle Head #1 Pd transfer
6 Ligands Execute Once Ligand transfer
1 Transfer Volumetrically Transfer liquid from Ligand1 to variable 'one_reaction' with Needle Head #1
2 Transfer Volumetrically Transfer liquid from Ligand2 to variable 'one_reaction' with Needle Head #1
3 Transfer Volumetrically Transfer liquid from Ligand3 to variable 'one_reaction' with Needle Head #1
4 Transfer Volumetrically Transfer liquid from Ligand4 to variable 'one_reaction' with Needle Head #1
5 Transfer Volumetrically Transfer liquid from Ligand5 to variable 'one_reaction' with Needle Head #1
6 Transfer Volumetrically Transfer liquid from Ligand6 to variable 'one_reaction' with Needle Head #1
7 Transfer Volumetrically Transfer liquid from Ligand7 to variable 'one_reaction' with Needle Head #1
8 Transfer Volumetrically Transfer liquid from Ligand8 to variable 'one_reaction' with Needle Head #1
9 Transfer Volumetrically Transfer liquid from Ligand9 to variable 'one_reaction' with Needle Head #1
10 Transfer Volumetrically Transfer liquid from Ligand10 to variable 'one_reaction' with Needle Head #1
11 Transfer Volumetrically Transfer liquid from Ligand11 to variable 'one_reaction' with Needle Head #1
12 Transfer Volumetrically Transfer liquid from Ligand12 to variable 'one_reaction' with Needle Head #1
13 Transfer Volumetrically Transfer liquid from Ligand13 to variable 'one_reaction' with Needle Head #1
14 Transfer Volumetrically Transfer liquid from Ligand14 to variable 'one_reaction' with Needle Head #1
15 Transfer Volumetrically Transfer liquid from Ligand15 to variable 'one_reaction' with Needle Head #1
16 Transfer Volumetrically Transfer liquid from Ligand16 to variable 'one_reaction' with Needle Head #1
17 Transfer Volumetrically Transfer liquid from Ligand17 to variable 'one_reaction' with Needle Head #1
18 Transfer Volumetrically Transfer liquid from Ligand18 to variable 'one_reaction' with Needle Head #1
19 Transfer Volumetrically Transfer liquid from Ligand19 to variable 'one_reaction' with Needle Head #1
20 Transfer Volumetrically Transfer liquid from Ligand20 to variable 'one_reaction' with Needle Head #1
21 Transfer Volumetrically Transfer liquid from Ligand21 to variable 'one_reaction' with Needle Head #1
22 Transfer Volumetrically Transfer liquid from Ligand22 to variable 'one_reaction' with Needle Head #1
23 Transfer Volumetrically Transfer liquid from Ligand23 to variable 'one_reaction' with Needle Head #1
24 Transfer Volumetrically Transfer liquid from valve ports C to Waste 1 with Needle Head #1
<insert sub tasks here>
7 Wait Waiting for 7:00 minutes
8 Transfer Volumetrically Transfer liquid from E-Tosyl_IS to variable 'one_reaction' with Needle Head #1 E-Tosylate transfer
9 Transfer Volumetrically Transfer liquid from ArBA to variable 'one_reaction' with Needle Head #1 ArBA transfer
10 Transfer Volumetrically Transfer liquid from ACN Anhydrous to variable 'one_reaction' with Needle He ACN transfer
11 Transfer Volumetrically Transfer liquid from valve ports C to Waste 1 with Needle Head #1
12 Log Data Log ''PdOAc2_vol=' + Pd_vol + '; E_Tosyl_IS_vol=' + E_Tosyl_IS_vol + '; ArBA_v
13 Set Variable reaction_t0 := Timestamp()
14 Transfer Volumetrically Transfer liquid from K3PO4 to variable 'one_reaction' with Needle Head #1 K3PO4 transfer
15 Export CSV 'Export in file 'Timestamp.csv''.
16 Log Data Log ''Reaction_t0=' + reaction_t0 + '; K3PO4_vol=' + K3PO4_vol + '; exit_code=
17 Set Variable Experiment_count := Experiment_count + 1
18 Set Variable reaction_count := reaction_count + 1
<insert sub tasks here>

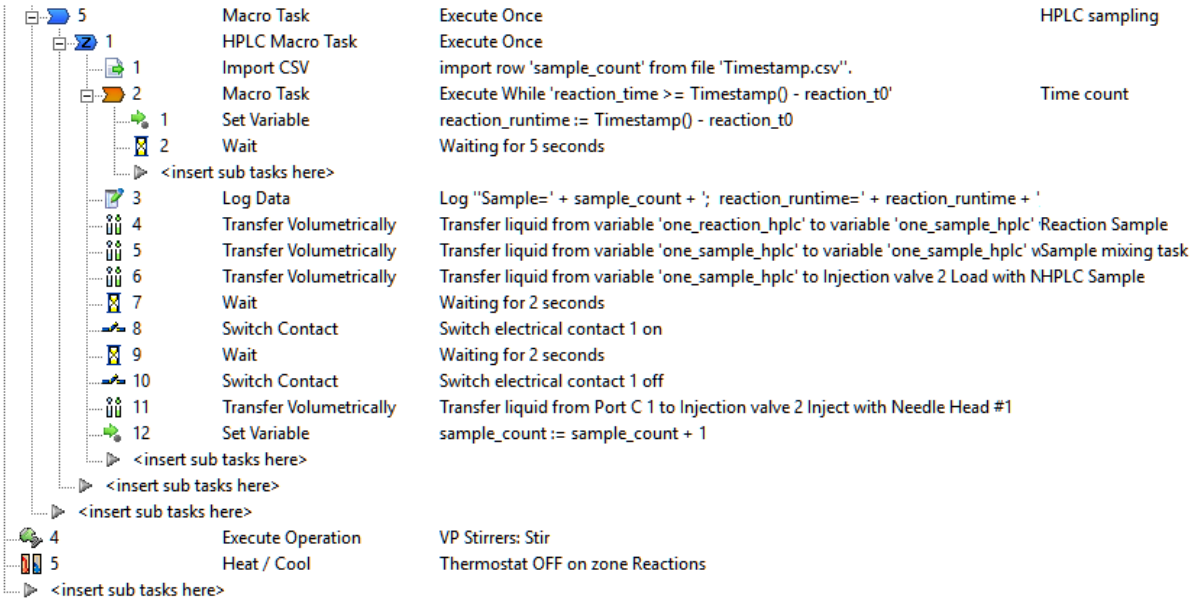


## 5. Machine learning algorithms

The ML algorithms used for experiment planning in this study, Phoenics[4] and Gryffin[5], leverage fundamental concepts from Bayesian optimization in combination with kernel density estimation. Bayesian optimization is an approach to global optimization for applications where the evaluation of a single parameter point is highly time or resource demanding. While several formulations exist, Bayesian optimization follows a two-step strategy to suggest parameter points for future evaluation: (1) constructing a statistical approximation to the considered experiment based on collected measurements, and (2) locating parameter points for which the approximation predicts promising performance. Phoenics and Gryffin construct the statistical approximation based on kernel density estimates of evaluated parameters and suggest promising parameter points with an explicit balance of exploitative and explorative sampling behavior with native support for batch optimization.

### 5.1 Process constrained optimization in the context of autonomous experimentation

The autonomous experimentation workflow described in the main text targeted the optimization of both processing conditions and categorical design choices with the goal to maximize the stereoselectivity of a Suzuki-Miyaura coupling reaction. One such reaction can be executed within about two hours on the employed Chemspeed system. However, the Chemspeed system offers the opportunity to run multiple reactions at once. With this parallelization capability, the overall runtime of an experimental campaign consisting of 192 experiments could, in principle, be reduced substantially.

Executing multiple reactions on this system simultaneously introduces a critical limitation to the decision-making process concerning the suggestion of promising reaction parameters: the temperature can only be controlled collectively for all concurrent reactions as opposed to an independent control for all other reaction parameters. This limitation requires adaptations to the decision-making algorithm to account for this process constraint.

For a mathematical formulation of this adaption, we consider a parameter domain $X$, which we can split into a domain Xc on which parameters are process constrained and a domain Xuc on which parameters are not process constrained, such that $X = X^c \cup X^{uc}$. The basic process constrained batch algorithm implemented in this study is inspired by a previously reported algorithm.[6] Following the aforementioned partitioning of the parameter domain, we first search for promising values for the constrained parameter values $x^c \in X^c$, for which we marginalize the collected feedback onto the $X^c$ domain. Subsequently, we search for promising parameter choices for $x^{uc} \in X^{uc}$ while considering the feedback on the entire domain $X$ given the specific choice of $x^c$ which we determined in the first step. Implementing this process in the kernel-based Bayesian optimization framework provided by Phoenics allows us to choose different sampling policies for the constrained and the unconstrained parameters. In this study, we choose two sampling policies for the constrained parameter and eight policies for the unconstrained parameters to reflect the fact that we executed eight reactions simultaneously.

## 6. Analytical data

### 6.1 $^1$H NMR weight % purity determinations

Vinyl tosylate **1-*E***, coupled product **2-*E***, and coupled product **2-*Z*** were assayed for weight % purity by $^1$H NMR against an internal standard of known weight and purity (99% 1,3,5-trimethoxybenzene). The tables and figures below show the weight % purity calculations and associated $^1$H NMR spectra.

**Table SI-6: Weight % purity calculation for 1-*E***

| | Peak Area (counts) | Protons (#) | Weight (mg) | MW (g/mol) | Purity (wt%) |
|---|---|---|---|---|---|
| Standard | 5.30 | 3 | 19.75 | 168.19 | 99% |
| Product | 2.02 | 2 | 21.41 | 310.36 | 96% |

**Table SI-7: Weight % purity calculation for 2-*E***

| | Peak Area (counts) | Protons (#) | Weight (mg) | MW (g/mol) | Purity (wt%) |
|---|---|---|---|---|---|
| Standard | 5.35 | 3 | 19.83 | 168.19 | 99% |
| Product | 2.03 | 2 | 22.75 | 322.40 | 94% |

**Table SI-8: Weight % purity calculation for 2-*Z***

| | Peak Area (counts) | Protons (#) | Weight (mg) | MW (g/mol) | Purity (wt%) |
|---|---|---|---|---|---|
| Standard | 5.26 | 3 | 17.90 | 168.19 | 99% |
| Product | 1.96 | 2 | 19.55 | 322.40 | 97% |

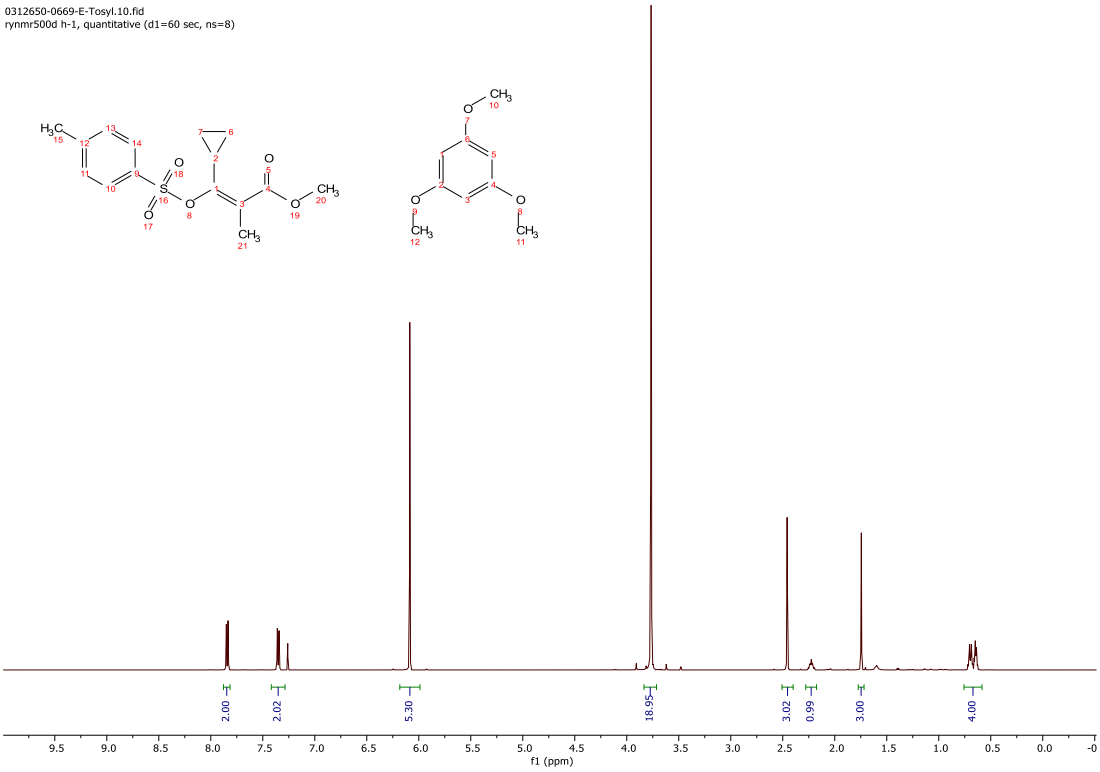


**Figure SI-5: $^{1}$H NMR for weight % purity determination of vinyl tosylate 1-*E***

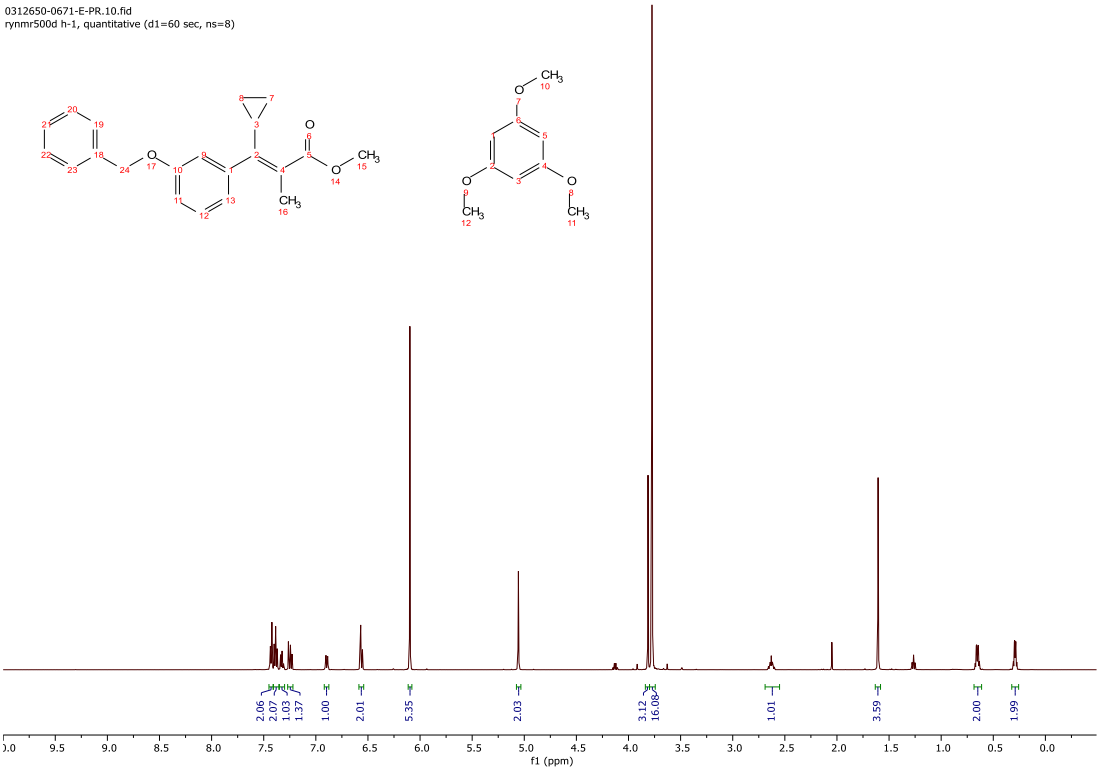


**Figure SI-6: $^{1}$H NMR for weight % purity determination of Suzuki product 2-*E***

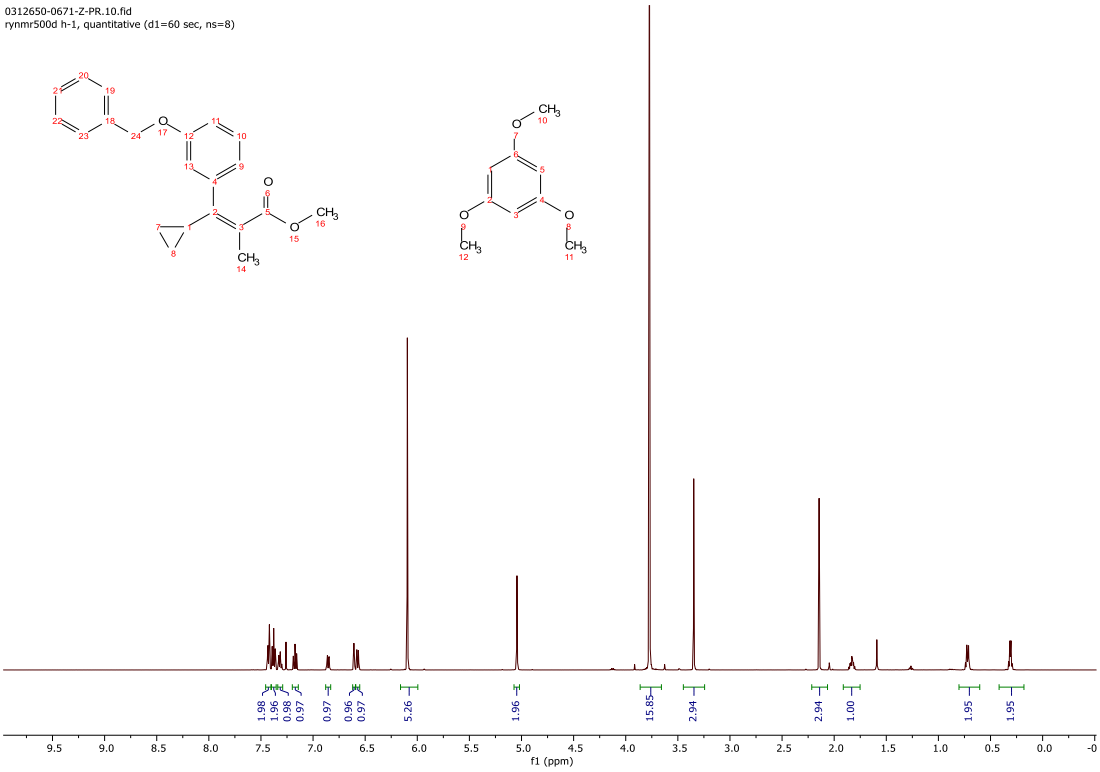


**Figure SI-7: $^{1}$H NMR for weight % purity determination of Suzuki product 2-*Z***

6.2 Calibration curves

HPLC-UV calibration curves were generated to determine the mol % distribution of reaction components **1-*E***, **2-*E*** and **2-*Z*** through measuring the ratio of their peak areas to an internal standard (**IS**) peak area (10 mol% 1,3,5-trimethoxybenzene). Thus, four mixtures were prepared containing 10 mol% **IS** and 100, 75, 50 or 25 mol% of each compound. Each mixture was acquired on the Chemspeed online HPLC system at 210 nm in duplicate. The mol% of compound in each mixture was plotted against the measured peak area ratio of each compound to **IS**, generating the calibration curves provided in figure SI-8. Linear regression with the intercept set at zero allowed for the determination of response factors for straightforward conversion of compound to **IS** ratio to mol % compound through the following equation: mol % compound = m * peak area of compound at 210 nm / peak area of **IS** at 210 nm, where m = the response factor determined through calibration. These response factors were included in the Python script for automated calculation of mol % compound from the HPLC data.

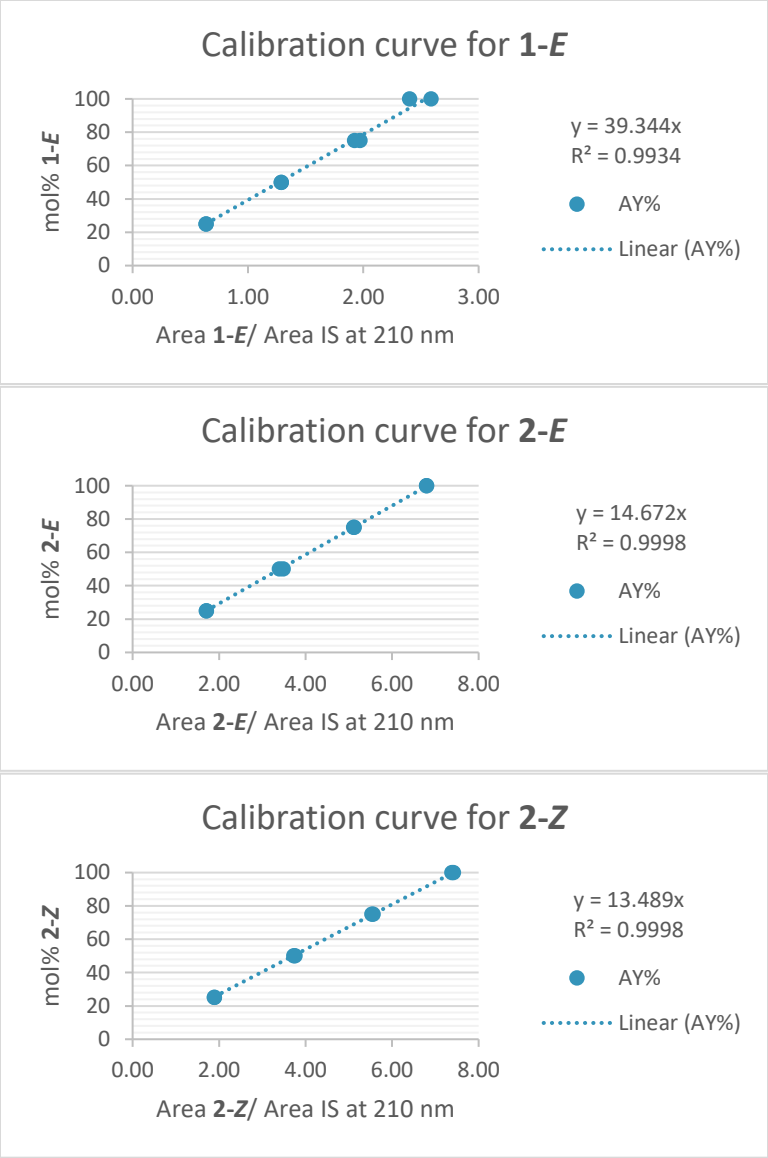


**Figure SI-8: Calibration curves for conversion of compound (1-*E*, 2-*E*, 2-*Z*) to internal standard (IS) HPLC area ratios at 210 nm to mol % distribution in the reaction mixture.**

6.3 Preliminary data

**Table SI-9: Reaction conditions and data included in Figure 1 of the main manuscript**

| Expt | Temp | Pd mol% | P ligand | P/Pd | ArBA eq. | 1-*E* mol% | 2-*E* mol% | 2-*Z* mol% |
|---|---|---|---|---|---|---|---|---|
| 1 | 25.00 | 4.10 | None | 0.00 | 1.95 | 1 | 3 | 91 |
| 2 | 25.00 | 1.70 | L11 | 2.35 | 1.05 | 45 | 1 | 48 |
| 3 | 25.00 | 1.70 | L7 | 2.35 | 1.05 | 2 | 60 | 35 |

6.4 Campaign 1 data

**Table SI-10: Reaction conditions and data included in Figure 3 of the main manuscript**

| Expt | Temp | Pd mol% | P ligand | P/Pd | ArBA eq. | 1-*E* mol% | 2-*E* mol% | 2-*Z* mol% |
|---|---|---|---|---|---|---|---|---|
| 1 | 29.14 | 2.50 | L5 | 3.36 | 1.25 | 95 | 1 | 5 |
| 2 | 29.14 | 3.90 | L2 | 2.36 | 1.03 | 86 | 3 | 3 |
| 3 | 29.14 | 2.80 | L1 | 1.71 | 1.30 | 43 | 25 | 45 |
| 4 | 29.14 | 2.70 | L11 | 1.93 | 1.03 | 9 | 2 | 88 |
| 5 | 29.14 | 2.00 | L8 | 2.80 | 1.45 | 59 | 3 | 31 |
| 6 | 29.14 | 1.20 | L8 | 3.33 | 1.75 | 61 | 2 | 29 |
| 7 | 29.14 | 1.90 | L4 | 1.47 | 1.33 | 11 | 10 | 78 |
| 8 | 29.14 | 2.90 | L3 | 2.07 | 1.53 | 86 | 0 | 2 |
| 9 | 25.50 | 4.90 | L3 | 1.80 | 1.95 | 41 | 4 | 46 |
| 10 | 25.50 | 4.90 | L12 | 0.82 | 1.93 | 1 | 2 | 95 |
| 11 | 25.50 | 4.90 | L7 | 3.59 | 1.98 | 79 | 1 | 1 |
| 12 | 25.50 | 4.00 | L7 | 0.60 | 1.90 | 1 | 26 | 75 |
| 13 | 25.50 | 1.30 | L10 | 4.00 | 1.90 | 48 | 1 | 33 |
| 14 | 25.50 | 4.90 | L10 | 3.76 | 1.85 | 8 | 2 | 70 |
| 15 | 25.50 | 1.80 | L1 | 0.44 | 1.43 | 54 | 26 | 41 |
| 16 | 25.50 | 2.50 | L1 | 3.68 | 1.08 | 76 | 2 | 6 |
| 17 | 10.33 | 4.80 | L12 | 3.42 | 1.20 | 2 | 3 | 98 |
| 18 | 10.33 | 1.40 | L1 | 0.57 | 1.33 | 47 | 23 | 23 |
| 19 | 10.33 | 2.50 | L2 | 1.12 | 2.00 | 41 | 26 | 21 |
| 20 | 10.33 | 1.00 | L6 | 3.20 | 1.38 | 75 | 0 | 11 |
| 21 | 10.33 | 1.40 | L10 | 0.57 | 1.88 | 36 | 1 | 52 |
| 22 | 10.33 | 1.90 | L1 | 0.63 | 1.23 | 38 | 26 | 23 |
| 23 | 10.33 | 2.40 | L1 | 0.50 | 1.33 | 30 | 4 | 64 |
| 24 | 10.33 | 4.60 | L6 | 0.61 | 1.08 | 11 | 2 | 80 |
| 25 | 13.10 | 3.60 | L5 | 3.56 | 1.90 | 77 | 0 | 10 |
| 26 | 13.10 | 4.80 | L9 | 0.50 | 1.20 | 12 | 5 | 78 |
| 27 | 13.10 | 2.80 | L1 | 3.00 | 1.93 | 77 | 1 | 1 |
| 28 | 13.10 | 2.20 | L5 | 0.91 | 1.08 | 27 | 2 | 70 |
| 29 | 13.10 | 1.90 | L1 | 1.47 | 1.00 | 86 | 6 | 10 |
| 30 | 13.10 | 4.90 | L3 | 0.90 | 1.23 | 28 | 5 | 53 |
| 31 | 13.10 | 1.70 | L2 | 0.71 | 1.05 | 57 | 17 | 19 |
| 32 | 13.10 | 2.70 | L12 | 3.26 | 1.93 | 1 | 3 | 94 |
| 33 | 39.90 | 4.50 | L7 | 0.89 | 1.38 | 2 | 6 | 93 |
| 34 | 39.90 | 1.10 | L4 | 0.73 | 1.98 | 64 | 1 | 21 |
| 35 | 39.90 | 1.90 | L9 | 0.63 | 2.00 | 26 | 2 | 70 |

| | | | | | | | | |
|---|---|---|---|---|---|---|---|---|
| 36 | 39.90 | 5.00 | L10 | 0.56 | 1.48 | 1 | 3 | 87 |
| 37 | 39.90 | 4.10 | L9 | 3.71 | 1.60 | 76 | 3 | 4 |
| 38 | 39.90 | 2.40 | L12 | 1.17 | 1.95 | 3 | 2 | 92 |
| 39 | 39.90 | 4.90 | L4 | 3.18 | 1.55 | 76 | 1 | 9 |
| 40 | 39.90 | 3.50 | L1 | 1.03 | 2.00 | 10 | 35 | 40 |
| 41 | 12.00 | 3.50 | L9 | 2.29 | 1.43 | 30 | 8 | 61 |
| 42 | 12.00 | 1.90 | L11 | 0.42 | 1.25 | 37 | 1 | 62 |
| 43 | 12.00 | 2.20 | L7 | 1.45 | 1.90 | 12 | 32 | 54 |
| 44 | 12.00 | 2.80 | L3 | 2.43 | 1.45 | 86 | 0 | 1 |
| 45 | 12.00 | 1.90 | L4 | 0.42 | 1.25 | 28 | 2 | 65 |
| 46 | 12.00 | 4.80 | L5 | 1.58 | 1.70 | 73 | 0 | 8 |
| 47 | 12.00 | 2.10 | L1 | 0.57 | 1.15 | 30 | 28 | 26 |
| 49 | 39.61 | 1.20 | L2 | 3.00 | 1.15 | 41 | 33 | 23 |
| 50 | 39.61 | 2.70 | L6 | 3.26 | 1.88 | 99 | 1 | 8 |
| 51 | 39.61 | 3.90 | L3 | 1.23 | 1.88 | 8 | 7 | 74 |
| 52 | 39.61 | 3.90 | L7 | 1.23 | 1.88 | 1 | 47 | 49 |
| 53 | 39.61 | 3.90 | L1 | 1.54 | 2.00 | 4 | 32 | 52 |
| 54 | 39.61 | 4.10 | L4 | 1.46 | 1.90 | 1 | 13 | 89 |
| 55 | 39.61 | 1.10 | L10 | 2.18 | 1.03 | 43 | 1 | 48 |
| 56 | 39.61 | 2.30 | L11 | 4.00 | 1.93 | 8 | 3 | 95 |
| 57 | 39.58 | 3.90 | L1 | 3.69 | 1.15 | 49 | 6 | 19 |
| 58 | 39.58 | 1.30 | L11 | 1.85 | 1.65 | 76 | 1 | 34 |
| 59 | 39.58 | 4.30 | L7 | 3.53 | 1.03 | 83 | 1 | 1 |
| 60 | 39.58 | 4.60 | L7 | 1.22 | 1.80 | 1 | 31 | 70 |
| 61 | 39.58 | 4.30 | L10 | 4.00 | 1.03 | 3 | 1 | 45 |
| 62 | 39.58 | 4.10 | L7 | 1.37 | 1.90 | 1 | 49 | 61 |
| 63 | 39.58 | 3.40 | L7 | 1.88 | 1.80 | 2 | 51 | 44 |
| 64 | 39.58 | 4.60 | L7 | 1.22 | 1.80 | 1 | 38 | 61 |
| 65 | 24.47 | 1.00 | L6 | 0.80 | 1.90 | 65 | 0 | 18 |
| 66 | 24.47 | 4.60 | L4 | 3.83 | 1.35 | 93 | 0 | 2 |
| 67 | 24.47 | 1.00 | L3 | 0.80 | 1.90 | 83 | 0 | 19 |
| 68 | 24.47 | 3.40 | L2 | 4.00 | 1.55 | 109 | 0 | 0 |
| 69 | 24.47 | 4.60 | L6 | 3.83 | 1.35 | 77 | 0 | 11 |
| 70 | 24.47 | 4.00 | L7 | 1.00 | 1.98 | 1 | 41 | 55 |
| 71 | 24.47 | 4.60 | L11 | 3.39 | 1.38 | 1 | 3 | 96 |
| 72 | 24.47 | 4.50 | L8 | 3.38 | 1.40 | 86 | 1 | 2 |
| 73 | 35.96 | 4.20 | L11 | 2.38 | 1.33 | 2 | 2 | 63 |
| 74 | 35.96 | 3.20 | L7 | 2.00 | 1.68 | 2 | 48 | 48 |
| 75 | 35.96 | 3.80 | L5 | 2.53 | 1.38 | 90 | 1 | 4 |
| 76 | 35.96 | 3.10 | L8 | 2.06 | 1.73 | 35 | 5 | 54 |
| 77 | 35.96 | 3.50 | L4 | 2.06 | 1.73 | 6 | 11 | 80 |
| 78 | 35.96 | 3.00 | L1 | 2.13 | 1.88 | 14 | 24 | 47 |
| 79 | 35.96 | 1.70 | L8 | 0.47 | 1.55 | 60 | 1 | 39 |

| | | | | | | | | |
|---|---|---|---|---|---|---|---|---|
| 80 | 35.96 | 2.30 | L12 | 0.70 | 1.53 | 12 | 2 | 89 |
| 81 | 30.03 | 1.20 | L4 | 2.00 | 2.00 | 29 | 7 | 51 |
| 82 | 30.03 | 1.20 | L7 | 2.00 | 2.00 | 68 | 12 | 50 |
| 83 | 30.03 | 3.40 | L7 | 1.65 | 1.75 | 2 | 45 | 58 |
| 84 | 30.03 | 3.90 | L3 | 0.51 | 1.05 | 17 | 5 | 71 |
| 85 | 30.03 | 3.80 | L7 | 2.74 | 1.70 | 50 | 17 | 16 |
| 86 | 30.03 | 3.80 | L5 | 0.74 | 1.03 | 3 | 3 | 92 |
| 87 | 30.03 | 3.90 | L11 | 0.62 | 1.50 | 1 | 3 | 98 |
| 88 | 30.03 | 4.80 | L10 | 2.00 | 1.55 | 1 | 3 | 78 |
| 89 | 36.51 | 3.00 | L7 | 1.87 | 2.00 | 3 | 46 | 38 |
| 90 | 36.51 | 3.80 | L5 | 3.89 | 1.98 | 102 | 1 | 4 |
| 91 | 36.51 | 2.80 | L7 | 2.86 | 1.73 | 14 | 45 | 34 |
| 92 | 36.51 | 1.60 | L3 | 1.00 | 1.03 | 44 | 3 | 45 |
| 93 | 36.51 | 3.00 | L7 | 1.87 | 2.00 | 2 | 59 | 46 |
| 94 | 36.51 | 1.30 | L12 | 4.00 | 1.38 | 40 | 2 | 66 |
| 95 | 36.51 | 4.60 | L3 | 2.87 | 1.98 | 101 | 0 | 2 |
| 96 | 36.51 | 2.30 | L7 | 2.09 | 1.63 | 1 | 52 | 44 |
| 97 | 12.39 | 2.90 | L12 | 3.17 | 1.03 | 17 | 2 | 68 |
| 98 | 12.39 | 1.30 | L5 | 2.46 | 2.00 | 72 | 0 | 7 |
| 99 | 12.39 | 2.40 | L4 | 1.50 | 1.80 | 49 | 5 | 43 |
| 100 | 12.39 | 2.90 | L7 | 3.31 | 1.03 | 87 | 0 | 0 |
| 101 | 12.39 | 4.50 | L4 | 1.96 | 1.03 | 59 | 4 | 31 |
| 102 | 12.39 | 3.50 | L6 | 0.69 | 1.63 | 19 | 2 | 74 |
| 103 | 12.39 | 3.10 | L4 | 3.48 | 1.10 | 91 | 0 | 1 |
| 104 | 12.39 | 1.30 | L7 | 3.08 | 1.83 | 50 | 28 | 14 |
| 105 | 35.27 | 2.10 | L7 | 2.67 | 1.03 | 2 | 40 | 40 |
| 106 | 35.27 | 2.00 | L1 | 2.00 | 1.63 | 30 | 20 | 39 |
| 107 | 35.27 | 2.80 | L3 | 3.86 | 1.48 | 91 | 0 | 1 |
| 108 | 35.27 | 2.20 | L4 | 2.00 | 1.65 | 2 | 13 | 90 |
| 109 | 35.27 | 4.80 | L8 | 1.50 | 1.15 | 17 | 6 | 69 |
| 110 | 35.27 | 3.30 | L12 | 1.70 | 2.00 | 1 | 4 | 104 |
| 111 | 35.27 | 3.00 | L11 | 4.00 | 1.33 | 2 | 3 | 90 |
| 112 | 35.27 | 2.80 | L5 | 3.86 | 1.48 | 74 | 0 | 4 |
| 113 | 23.50 | 1.00 | L12 | 2.40 | 1.13 | 59 | 0 | 22 |
| 114 | 23.50 | 2.80 | L11 | 2.29 | 1.98 | 17 | 3 | 89 |
| 115 | 23.50 | 1.10 | L10 | 2.91 | 1.08 | 55 | 1 | 32 |
| 116 | 23.50 | 3.70 | L7 | 1.51 | 1.93 | 2 | 56 | 39 |
| 117 | 23.50 | 1.10 | L2 | 2.91 | 1.05 | 103 | 0 | 0 |
| 118 | 23.50 | 3.70 | L7 | 1.51 | 1.93 | 2 | 65 | 42 |
| 119 | 23.50 | 1.10 | L7 | 2.91 | 1.08 | 1 | 57 | 34 |
| 120 | 23.50 | 2.30 | L6 | 0.52 | 1.03 | 26 | 2 | 63 |

6.5 Campaign 2 data

**Table SI-11: Reaction conditions and data included in Figure 5 of the main manuscript**

| Expt | Temp | Pd mol% | P ligand | P/Pd | 1-*E* mol% | 2-*E* mol% | 2-*Z* mol% |
|---|---|---|---|---|---|---|---|
| 9 | 32.81 | 2.70 | L31 | 2.59 | 85 | 17 | 6 |
| 10 | 32.81 | 1.30 | L30 | 1.69 | 35 | 51 | 20 |
| 11 | 32.81 | 2.80 | L29 | 2.86 | 77 | 1 | 5 |
| 12 | 32.81 | 1.80 | L22 | 1.67 | 55 | 15 | 34 |
| 13 | 32.81 | 3.40 | L12 | 1.88 | 1 | 2 | 99 |
| 14 | 32.81 | 1.90 | L29 | 3.26 | 87 | 0 | 3 |
| 15 | 32.81 | 1.90 | L13 | 1.58 | 74 | 16 | 16 |
| 16 | 32.81 | 2.00 | L27 | 1.60 | 13 | 8 | 85 |
| 17 | 35.15 | 1.00 | L30 | 4.00 | 48 | 45 | 17 |
| 18 | 35.15 | 4.80 | L20 | 3.79 | 30 | 34 | 40 |
| 19 | 35.15 | 4.20 | L15 | 3.90 | 106 | 0 | 0 |
| 20 | 35.15 | 1.40 | L30 | 0.57 | 20 | 38 | 48 |
| 21 | 35.15 | 5.00 | L16 | 3.68 | 104 | 1 | 1 |
| 22 | 35.15 | 4.30 | L30 | 0.60 | 1 | 58 | 46 |
| 23 | 35.15 | 1.30 | L30 | 2.00 | 27 | 57 | 22 |
| 24 | 35.15 | 5.00 | L26 | 3.92 | 1 | 51 | 54 |
| 25 | 10.37 | 1.00 | L4 | 0.60 | 43 | 2 | 67 |
| 26 | 10.37 | 1.00 | L32 | 0.60 | 93 | 6 | 10 |
| 27 | 10.37 | 4.70 | L2 | 2.43 | 107 | 1 | 0 |
| 28 | 10.37 | 1.20 | L21 | 4.00 | 108 | 1 | 0 |
| 29 | 10.37 | 1.80 | L18 | 3.89 | 106 | 0 | 0 |
| 30 | 10.37 | 4.80 | L17 | 1.88 | 88 | 9 | 9 |
| 31 | 10.37 | 4.80 | L24 | 1.17 | 69 | 18 | 17 |
| 32 | 10.37 | 5.00 | L19 | 1.44 | 69 | 8 | 30 |
| 33 | 36.37 | 4.50 | L30 | 0.76 | 4 | 63 | 41 |
| 34 | 36.37 | 5.00 | L25 | 2.32 | 4 | 30 | 65 |
| 35 | 36.37 | 5.00 | L19 | 2.32 | 108 | 0 | 0 |
| 36 | 36.37 | 1.40 | L30 | 2.86 | 28 | 57 | 22 |
| 37 | 36.37 | 3.30 | L25 | 0.55 | 8 | 34 | 67 |
| 38 | 36.37 | 1.30 | L30 | 2.62 | 25 | 60 | 23 |
| 39 | 36.37 | 4.90 | L14 | 0.94 | 1 | 3 | 101 |
| 40 | 36.37 | 1.60 | L30 | 2.63 | 27 | 58 | 22 |
| 41 | 14.32 | 4.50 | L23 | 3.78 | 109 | 3 | 3 |
| 42 | 14.32 | 3.00 | L14 | 1.27 | 7 | 3 | 98 |
| 43 | 14.32 | 2.30 | L24 | 2.17 | 108 | 0 | 0 |
| 44 | 14.32 | 2.70 | L27 | 1.63 | 42 | 5 | 62 |
| 45 | 14.32 | 4.40 | L16 | 1.14 | 11 | 6 | 89 |

| | | | | | | | |
|---|---|---|---|---|---|---|---|
| 46 | 14.32 | 3.80 | L32 | 3.95 | 106 | 0 | 0 |
| 47 | 14.32 | 2.60 | L28 | 2.08 | 106 | 0 | 1 |
| 48 | 14.32 | 3.20 | L29 | 1.06 | 67 | 1 | 24 |
| 49 | 37.96 | 1.10 | L30 | 2.73 | 36 | 54 | 21 |
| 50 | 37.96 | 1.10 | L2 | 2.91 | 75 | 20 | 12 |
| 51 | 37.96 | 1.10 | L21 | 2.73 | 84 | 7 | 15 |
| 52 | 37.96 | 1.10 | L24 | 2.91 | 102 | 1 | 2 |
| 53 | 37.96 | 1.00 | L30 | 2.60 | 36 | 51 | 19 |
| 54 | 37.96 | 1.10 | L4 | 2.91 | 64 | 5 | 35 |
| 55 | 37.96 | 2.20 | L17 | 0.55 | 4 | 10 | 92 |
| 56 | 37.96 | 1.10 | L14 | 2.73 | 29 | 2 | 77 |
| 57 | 22.52 | 1.10 | L14 | 3.09 | 32 | 2 | 84 |
| 58 | 22.52 | 1.10 | L30 | 0.91 | 55 | 37 | 17 |
| 59 | 22.52 | 4.60 | L28 | 0.83 | 28 | 2 | 76 |
| 60 | 22.52 | 1.00 | L19 | 2.80 | 107 | 0 | 0 |
| 61 | 22.52 | 1.20 | L12 | 3.17 | 14 | 2 | 91 |
| 62 | 22.52 | 4.10 | L30 | 0.59 | 5 | 56 | 43 |
| 63 | 22.52 | 1.10 | L25 | 3.09 | 107 | 0 | 1 |
| 64 | 22.52 | 1.00 | L30 | 2.80 | 61 | 34 | 13 |
| 65 | 25.98 | 4.70 | L30 | 0.85 | 9 | 65 | 33 |
| 66 | 25.98 | 4.60 | L18 | 2.43 | 100 | 0 | 4 |
| 67 | 25.98 | 4.20 | L4 | 3.14 | 105 | 0 | 3 |
| 68 | 25.98 | 2.80 | L28 | 3.93 | 105 | 1 | 1 |
| 69 | 25.98 | 4.10 | L13 | 3.17 | 106 | 0 | 0 |
| 70 | 25.98 | 3.10 | L32 | 4.00 | 103 | 2 | 2 |
| 71 | 25.98 | 4.20 | L22 | 3.24 | 99 | 1 | 5 |
| 72 | 25.98 | 3.70 | L30 | 0.76 | 9 | 62 | 34 |
| 73 | 27.45 | 4.70 | L30 | 0.81 | 7 | 63 | 37 |
| 74 | 27.45 | 3.30 | L21 | 0.97 | 38 | 39 | 26 |
| 75 | 27.45 | 3.40 | L12 | 0.53 | 4 | 3 | 103 |
| 76 | 27.45 | 3.40 | L18 | 0.65 | 19 | 16 | 70 |
| 77 | 27.45 | 3.20 | L32 | 0.81 | 48 | 28 | 29 |
| 78 | 27.45 | 3.40 | L4 | 0.76 | 10 | 9 | 85 |
| 79 | 27.45 | 5.00 | L26 | 1.08 | 1 | 41 | 62 |
| 80 | 27.45 | 5.00 | L23 | 1.04 | 77 | 4 | 27 |
| 81 | 27.40 | 4.20 | L30 | 1.38 | 5 | 72 | 30 |
| 82 | 27.40 | 1.40 | L19 | 0.57 | 13 | 10 | 85 |
| 83 | 27.40 | 3.60 | L30 | 0.94 | 12 | 64 | 29 |
| 84 | 27.40 | 3.30 | L25 | 1.94 | 38 | 23 | 40 |
| 85 | 27.40 | 1.70 | L29 | 0.59 | 16 | 2 | 82 |
| 86 | 27.40 | 1.70 | L16 | 0.59 | 19 | 5 | 84 |
| 87 | 27.40 | 4.80 | L22 | 0.75 | 33 | 27 | 44 |
| 88 | 27.40 | 3.60 | L31 | 2.39 | 75 | 20 | 8 |

| | | | | | | | |
|---|---|---|---|---|---|---|---|
| 89 | 10.11 | 4.60 | L24 | 0.87 | 66 | 22 | 19 |
| 90 | 10.11 | 1.00 | L30 | 2.20 | 87 | 14 | 5 |
| 91 | 10.11 | 3.10 | L15 | 2.97 | 108 | 0 | 0 |
| 92 | 10.11 | 3.10 | L31 | 3.16 | 106 | 2 | 1 |
| 93 | 10.11 | 1.10 | L31 | 2.73 | 107 | 1 | 0 |
| 94 | 10.11 | 1.00 | L13 | 1.80 | 93 | 5 | 9 |
| 95 | 10.11 | 1.00 | L20 | 1.80 | 98 | 4 | 5 |
| 96 | 10.11 | 3.60 | L30 | 3.06 | 74 | 21 | 9 |
| 105 | 22.38 | 2.50 | L16 | 2.72 | 42 | 7 | 60 |
| 106 | 22.38 | 1.40 | L22 | 1.71 | 75 | 11 | 19 |
| 107 | 22.38 | 3.80 | L30 | 0.74 | 16 | 55 | 34 |
| 108 | 22.38 | 4.80 | L30 | 0.71 | 8 | 59 | 37 |
| 109 | 22.38 | 4.70 | L30 | 1.62 | 28 | 55 | 22 |
| 110 | 22.38 | 2.00 | L20 | 1.70 | 26 | 35 | 45 |
| 111 | 22.38 | 1.30 | L23 | 1.69 | 105 | 2 | 4 |
| 112 | 22.38 | 4.70 | L30 | 1.57 | 26 | 57 | 23 |
| 113 | 27.86 | 4.20 | L30 | 1.52 | 16 | 64 | 26 |
| 114 | 27.86 | 1.70 | L32 | 3.88 | 103 | 2 | 2 |
| 115 | 27.86 | 1.70 | L26 | 3.88 | 30 | 38 | 39 |
| 116 | 27.86 | 1.60 | L17 | 3.88 | 108 | 0 | 0 |
| 117 | 27.86 | 4.40 | L30 | 1.59 | 11 | 67 | 27 |
| 118 | 27.86 | 3.90 | L30 | 1.69 | 13 | 66 | 26 |
| 119 | 27.86 | 1.60 | L19 | 4.00 | 107 | 0 | 0 |
| 120 | 27.86 | 4.00 | L30 | 1.50 | 13 | 66 | 27 |
| 121 | 39.07 | 4.10 | L19 | 0.54 | 3 | 28 | 76 |
| 122 | 39.07 | 4.80 | L30 | 0.63 | 1 | 61 | 43 |
| 123 | 39.07 | 4.40 | L30 | 0.68 | 1 | 64 | 40 |
| 124 | 39.07 | 3.30 | L20 | 3.94 | 31 | 33 | 40 |
| 125 | 39.07 | 2.60 | L31 | 4.00 | 71 | 23 | 7 |
| 126 | 39.07 | 2.60 | L26 | 3.85 | 9 | 46 | 50 |
| 127 | 39.07 | 2.90 | L16 | 3.93 | 106 | 0 | 0 |
| 128 | 39.07 | 2.70 | L2 | 4.00 | 100 | 5 | 3 |
| 129 | 31.77 | 4.10 | L30 | 2.05 | 10 | 69 | 28 |
| 130 | 31.77 | 4.40 | L21 | 1.86 | 18 | 46 | 41 |
| 131 | 31.77 | 4.80 | L29 | 3.08 | 59 | 0 | 4 |
| 132 | 31.77 | 4.20 | L30 | 1.95 | 7 | 69 | 28 |
| 133 | 31.77 | 4.10 | L30 | 2.05 | 11 | 67 | 27 |
| 134 | 31.77 | 4.10 | L30 | 2.05 | 8 | 69 | 28 |
| 135 | 31.77 | 4.80 | L23 | 3.08 | 99 | 3 | 6 |
| 136 | 31.77 | 4.10 | L30 | 1.90 | 6 | 72 | 29 |
| 137 | 17.56 | 4.90 | L30 | 2.08 | 49 | 41 | 17 |
| 138 | 17.56 | 4.70 | L30 | 0.51 | 22 | 46 | 37 |
| 139 | 17.56 | 4.00 | L13 | 2.05 | 99 | 5 | 3 |

| | | | | | | | |
|---|---|---|---|---|---|---|---|
| 140 | 17.56 | 3.70 | L25 | 2.59 | 75 | 12 | 18 |
| 141 | 17.56 | 1.90 | L24 | 0.63 | 47 | 30 | 30 |
| 142 | 17.56 | 1.90 | L15 | 0.53 | 21 | 14 | 71 |
| 143 | 17.56 | 3.80 | L23 | 2.00 | 99 | 3 | 5 |
| 144 | 17.56 | 1.90 | L25 | 0.63 | 38 | 18 | 52 |
| 145 | 33.85 | 4.10 | L12 | 2.83 | 1 | 3 | 98 |
| 146 | 33.85 | 4.20 | L30 | 1.81 | 4 | 71 | 29 |
| 147 | 33.85 | 3.80 | L30 | 1.74 | 7 | 68 | 27 |
| 148 | 33.85 | 3.80 | L13 | 2.63 | 107 | 0 | 0 |
| 149 | 33.85 | 3.90 | L4 | 3.13 | 100 | 1 | 6 |
| 150 | 33.85 | 3.60 | L4 | 3.22 | 100 | 1 | 7 |
| 151 | 33.85 | 3.90 | L28 | 3.13 | 98 | 4 | 2 |
| 152 | 33.85 | 4.50 | L30 | 1.87 | 1 | 73 | 30 |
| 153 | 16.67 | 2.80 | L22 | 4.00 | 109 | 0 | 0 |
| 154 | 16.67 | 5.00 | L14 | 3.12 | 10 | 3 | 93 |
| 155 | 16.67 | 2.80 | L4 | 4.00 | 106 | 0 | 1 |
| 156 | 16.67 | 4.90 | L15 | 0.65 | 13 | 28 | 64 |
| 157 | 16.67 | 2.80 | L23 | 3.86 | 104 | 2 | 3 |
| 158 | 16.67 | 4.20 | L30 | 0.57 | 22 | 50 | 33 |
| 159 | 16.67 | 5.00 | L28 | 3.04 | 106 | 0 | 0 |
| 160 | 16.67 | 5.00 | L27 | 3.24 | 49 | 10 | 59 |
| 161 | 35.05 | 3.80 | L30 | 2.42 | 6 | 73 | 29 |
| 162 | 35.05 | 4.50 | L30 | 2.31 | 3 | 72 | 29 |
| 163 | 35.05 | 3.80 | L30 | 1.21 | 3 | 73 | 31 |
| 164 | 35.05 | 4.50 | L30 | 2.31 | 1 | 73 | 30 |
| 165 | 35.05 | 4.00 | L31 | 1.05 | 40 | 19 | 42 |
| 166 | 35.05 | 4.20 | L30 | 1.81 | 2 | 72 | 29 |
| 167 | 35.05 | 1.70 | L17 | 2.47 | 107 | 0 | 0 |
| 168 | 35.05 | 1.70 | L23 | 2.24 | 102 | 2 | 4 |
| 169 | 11.26 | 4.20 | L13 | 0.52 | 35 | 15 | 58 |
| 170 | 11.26 | 2.00 | L30 | 2.90 | 82 | 18 | 7 |
| 171 | 11.26 | 1.90 | L2 | 1.05 | 67 | 25 | 14 |
| 172 | 11.26 | 3.90 | L18 | 1.49 | 72 | 10 | 24 |
| 173 | 11.26 | 3.90 | L26 | 1.49 | 16 | 42 | 48 |
| 174 | 11.26 | 2.00 | L30 | 2.90 | 83 | 18 | 7 |
| 175 | 11.26 | 2.20 | L12 | 2.91 | 7 | 2 | 96 |
| 176 | 11.26 | 4.60 | L30 | 0.61 | 33 | 46 | 27 |
| 177 | 29.84 | 1.10 | L4 | 2.55 | 87 | 3 | 20 |
| 178 | 29.84 | 4.10 | L2 | 1.22 | 30 | 45 | 31 |
| 179 | 29.84 | 3.90 | L27 | 1.49 | 6 | 10 | 89 |
| 180 | 29.84 | 1.10 | L18 | 2.55 | 104 | 0 | 2 |
| 181 | 29.84 | 1.90 | L21 | 2.32 | 98 | 3 | 5 |
| 182 | 29.84 | 4.20 | L16 | 1.48 | 14 | 9 | 80 |

| | | | | | | | |
|---|---|---|---|---|---|---|---|
| 183 | 29.84 | 1.80 | L15 | 2.44 | 56 | 13 | 37 |
| 184 | 29.84 | 3.80 | L30 | 1.74 | 13 | 68 | 28 |
| 185 | 21.92 | 3.20 | L26 | 2.06 | 7 | 49 | 53 |
| 186 | 21.92 | 4.30 | L30 | 0.98 | 19 | 59 | 25 |
| 187 | 21.92 | 3.00 | L17 | 1.40 | 72 | 12 | 22 |
| 188 | 21.92 | 3.00 | L12 | 1.40 | 1 | 3 | 99 |
| 189 | 21.92 | 3.00 | L31 | 1.40 | 48 | 9 | 50 |
| 190 | 21.92 | 4.60 | L13 | 1.43 | 51 | 24 | 28 |
| 191 | 21.92 | 2.60 | L22 | 1.00 | 63 | 16 | 25 |
| 192 | 21.92 | 4.80 | L27 | 1.38 | 13 | 8 | 85 |

6.6 Campaign 3 data

Campaign 3 incorporated 15 manually selected computed phosphine descriptors into the algorithmic optimization to relate ligands among one another with respect to steric and electronic features. The selected properties and the computed values for each ligand are provided in the attachment below.

200127_Ligand_properties_campaign_3.

**Table SI-12: Reaction conditions and data included in Figure SI-9**

| **Expt** | **Temp** | **Pd mol%** | **P ligand** | **P/Pd** | **1-*E* mol%** | **2-*E* mol%** | **2-*Z* mol%** |
|---|---|---|---|---|---|---|---|
| 9 | 32.81 | 2.00 | L27 | 1.60 | 12 | 6 | 86 |
| 10 | 32.81 | 1.90 | L29 | 3.26 | 69 | 1 | 7 |
| 11 | 32.81 | 2.80 | L29 | 2.86 | 66 | 1 | 7 |
| 12 | 32.81 | 2.70 | L31 | 2.59 | 63 | 23 | 8 |
| 13 | 32.81 | 1.30 | L30 | 1.69 | 23 | 56 | 24 |
| 14 | 32.81 | 1.90 | L13 | 1.58 | 46 | 23 | 29 |
| 15 | 32.81 | 1.80 | L22 | 1.67 | 40 | 18 | 12 |
| 16 | 32.81 | 3.40 | L12 | 1.88 | 6 | 3 | 92 |
| 17 | 27.45 | 4.90 | L32 | 3.10 | 87 | 8 | 7 |
| 18 | 27.45 | 1.00 | L31 | 1.20 | 41 | 5 | 56 |
| 19 | 27.45 | 4.80 | L14 | 3.83 | 1 | 3 | 94 |
| 20 | 27.45 | 1.10 | L4 | 0.73 | 10 | 3 | 88 |
| 21 | 27.45 | 1.20 | L24 | 0.67 | 26 | 33 | 44 |
| 22 | 27.45 | 4.80 | L16 | 0.83 | 1 | 8 | 86 |
| 23 | 27.45 | 2.10 | L27 | 0.86 | 2 | 4 | 95 |
| 24 | 27.45 | 1.10 | L19 | 0.73 | 13 | 13 | 74 |
| 25 | 10.15 | 1.50 | L26 | 3.87 | 35 | 36 | 35 |
| 26 | 10.15 | 2.20 | L12 | 3.45 | 3 | 5 | 93 |

| | | | | | | | |
|---|---|---|---|---|---|---|---|
| 27 | 10.15 | 4.80 | L31 | 1.25 | 60 | 7 | 33 |
| 28 | 10.15 | 1.40 | L19 | 2.57 | 105 | 0 | 0 |
| 29 | 10.15 | 4.30 | L14 | 0.51 | 6 | 3 | 92 |
| 30 | 10.15 | 2.20 | L16 | 3.82 | 46 | 5 | 50 |
| 31 | 10.15 | 4.70 | L28 | 0.64 | 11 | 2 | 88 |
| 32 | 10.15 | 1.50 | L13 | 3.73 | 101 | 0 | 0 |
| 33 | 31.07 | 1.30 | L27 | 2.31 | 16 | 6 | 82 |
| 34 | 31.07 | 3.40 | L16 | 3.29 | 36 | 8 | 55 |
| 35 | 31.07 | 3.50 | L26 | 3.94 | 1 | 45 | 54 |
| 36 | 31.07 | 1.10 | L20 | 2.00 | 11 | 50 | 51 |
| 37 | 31.07 | 3.30 | L14 | 3.82 | 6 | 3 | 91 |
| 38 | 31.07 | 1.30 | L2 | 2.15 | 34 | 39 | 26 |
| 39 | 31.07 | 1.00 | L4 | 2.00 | 24 | 9 | 69 |
| 40 | 31.07 | 1.10 | L19 | 2.18 | 53 | 17 | 30 |
| 41 | 11.12 | 5.00 | L12 | 3.56 | 3 | 3 | 95 |
| 42 | 11.12 | 1.80 | L23 | 4.00 | 97 | 2 | 4 |
| 43 | 11.12 | 4.70 | L16 | 3.02 | 28 | 6 | 66 |
| 44 | 11.12 | 1.50 | L16 | 0.67 | 21 | 3 | 77 |
| 45 | 11.12 | 1.50 | L30 | 4.00 | 79 | 16 | 6 |
| 46 | 11.12 | 2.00 | L26 | 0.60 | 22 | 24 | 55 |
| 47 | 11.12 | 2.00 | L14 | 0.70 | 8 | 3 | 90 |
| 48 | 11.12 | 1.70 | L26 | 3.88 | 28 | 37 | 36 |
| 49 | 28.03 | 2.70 | L30 | 3.70 | 20 | 65 | 23 |
| 50 | 28.03 | 3.20 | L26 | 3.56 | 1 | 47 | 53 |
| 51 | 28.03 | 3.40 | L16 | 0.88 | 2 | 16 | 87 |
| 52 | 28.03 | 2.80 | L28 | 3.71 | 97 | 2 | 1 |
| 53 | 28.03 | 3.50 | L14 | 0.57 | 1 | 3 | 96 |
| 54 | 28.03 | 4.00 | L26 | 3.95 | 1 | 46 | 54 |
| 55 | 28.03 | 3.50 | L14 | 3.89 | 5 | 13 | 90 |
| 56 | 28.03 | 4.00 | L28 | 3.95 | 97 | 2 | 1 |
| 57 | 15.81 | 3.60 | L26 | 2.33 | 5 | 44 | 54 |
| 58 | 15.81 | 3.00 | L16 | 2.07 | 14 | 11 | 78 |
| 59 | 15.81 | 1.20 | L14 | 3.67 | 17 | 2 | 82 |
| 60 | 15.81 | 3.10 | L31 | 2.00 | 37 | 5 | 59 |
| 61 | 15.81 | 1.20 | L23 | 3.67 | 95 | 2 | 4 |
| 62 | 15.81 | 1.90 | L28 | 3.89 | 101 | 0 | 0 |
| 63 | 15.81 | 3.20 | L17 | 2.19 | 80 | 9 | 11 |
| 64 | 15.81 | 3.20 | L13 | 2.06 | 64 | 17 | 17 |
| 65 | 23.80 | 3.40 | L30 | 3.53 | 27 | 54 | 22 |
| 66 | 23.80 | 4.20 | L28 | 3.86 | 101 | 1 | 1 |
| 67 | 23.80 | 4.80 | L26 | 1.67 | 1 | 39 | 59 |
| 68 | 23.80 | 1.90 | L27 | 3.68 | 30 | 12 | 64 |
| 69 | 23.80 | 2.00 | L29 | 3.80 | 77 | 2 | 6 |

| | | | | | | | |
|---|---|---|---|---|---|---|---|
| 70 | 23.80 | 2.30 | L22 | 3.74 | 65 | 8 | 25 |
| 71 | 23.80 | 4.90 | L16 | 2.29 | 8 | 8 | 81 |
| 72 | 23.80 | 2.30 | L16 | 2.35 | 25 | 7 | 68 |
| 73 | 38.76 | 4.90 | L16 | 3.71 | 28 | 12 | 59 |
| 74 | 38.76 | 3.50 | L26 | 3.89 | 2 | 44 | 54 |
| 75 | 38.76 | 4.80 | L17 | 1.71 | 24 | 35 | 39 |
| 76 | 38.76 | 3.60 | L31 | 3.94 | 51 | 30 | 10 |
| 77 | 38.76 | 4.90 | L13 | 1.59 | 11 | 41 | 43 |
| 78 | 38.76 | 4.90 | L23 | 1.06 | 43 | 4 | 52 |
| 79 | 38.76 | 3.50 | L28 | 3.54 | 86 | 7 | 2 |
| 80 | 38.76 | 1.10 | L2 | 1.27 | 13 | 49 | 37 |
| 81 | 21.11 | 3.20 | L32 | 3.81 | 96 | 1 | 1 |
| 82 | 21.11 | 3.00 | L16 | 1.07 | 18 | 6 | 77 |
| 83 | 21.11 | 3.30 | L13 | 3.64 | 102 | 0 | 0 |
| 84 | 21.11 | 3.50 | L22 | 3.31 | 49 | 13 | 35 |
| 85 | 21.11 | 3.30 | L27 | 3.64 | 27 | 8 | 72 |
| 86 | 21.11 | 3.30 | L19 | 3.64 | 103 | 0 | 0 |
| 87 | 21.11 | 3.20 | L4 | 3.69 | 99 | 1 | 2 |
| 88 | 21.11 | 1.00 | L16 | 2.40 | 45 | 5 | 53 |
| 89 | 38.19 | 1.10 | L2 | 0.73 | 11 | 48 | 43 |
| 90 | 38.19 | 3.00 | L16 | 0.73 | 1 | 10 | 86 |
| 91 | 38.19 | 1.40 | L27 | 0.86 | 3 | 4 | 87 |
| 92 | 38.19 | 1.10 | L19 | 0.55 | 6 | 2 | 91 |
| 93 | 38.19 | 1.00 | L32 | 1.40 | 43 | 29 | 27 |
| 94 | 38.19 | 1.00 | L31 | 1.40 | 57 | 8 | 36 |
| 95 | 38.19 | 3.00 | L12 | 0.73 | 5 | 3 | 94 |
| 96 | 38.19 | 2.90 | L14 | 0.97 | 2 | 3 | 97 |
| 105 | 10.72 | 3.20 | L24 | 0.88 | 50 | 29 | 24 |
| 106 | 10.72 | 3.60 | L23 | 3.78 | 97 | 2 | 4 |
| 107 | 10.72 | 4.00 | L30 | 2.70 | 59 | 30 | 12 |
| 108 | 10.72 | 3.20 | L16 | 0.50 | 16 | 3 | 79 |
| 109 | 10.72 | 3.80 | L28 | 2.89 | 101 | 0 | 0 |
| 110 | 10.72 | 3.30 | L14 | 1.15 | 8 | 2 | 90 |
| 111 | 10.72 | 3.80 | L14 | 2.89 | 16 | 2 | 82 |
| 112 | 10.72 | 3.80 | L26 | 2.16 | 14 | 41 | 47 |
| 113 | 29.63 | 2.90 | L16 | 1.59 | 59 | 12 | 35 |
| 114 | 29.63 | 2.60 | L14 | 2.15 | 6 | 3 | 89 |
| 115 | 29.63 | 2.40 | L27 | 3.83 | 13 | 10 | 80 |
| 116 | 29.63 | 4.00 | L13 | 2.65 | 100 | 0 | 0 |
| 117 | 29.63 | 3.40 | L26 | 3.65 | 1 | 46 | 54 |
| 118 | 29.63 | 2.40 | L32 | 3.83 | 93 | 11 | 2 |
| 119 | 29.63 | 2.40 | L22 | 3.67 | 40 | 13 | 43 |
| 120 | 29.63 | 3.50 | L28 | 3.37 | 96 | 2 | 1 |

| | | | | | | | |
|---|---|---|---|---|---|---|---|
| 121 | 15.13 | 3.90 | L30 | 2.36 | 48 | 38 | 15 |
| 122 | 15.13 | 3.50 | L26 | 2.80 | 8 | 45 | 49 |
| 123 | 15.13 | 1.40 | L26 | 1.57 | 24 | 38 | 42 |
| 124 | 15.13 | 4.00 | L28 | 2.50 | 100 | 3 | 0 |
| 125 | 15.13 | 1.10 | L16 | 1.45 | 36 | 3 | 65 |
| 126 | 15.13 | 1.40 | L24 | 1.57 | 77 | 13 | 12 |
| 127 | 15.13 | 1.30 | L28 | 1.38 | 100 | 1 | 2 |
| 128 | 15.13 | 3.80 | L14 | 2.53 | 6 | 3 | 91 |
| 129 | 34.30 | 4.20 | L23 | 0.52 | 2 | 4 | 93 |
| 130 | 34.30 | 4.20 | L14 | 0.57 | 6 | 3 | 93 |
| 131 | 34.30 | 5.00 | L16 | 2.36 | 12 | 11 | 72 |
| 132 | 34.30 | 1.20 | L22 | 1.67 | 49 | 18 | 12 |
| 133 | 34.30 | 4.00 | L26 | 0.70 | 1 | 29 | 70 |
| 134 | 34.30 | 4.20 | L28 | 3.86 | 90 | 7 | 2 |
| 135 | 34.30 | 4.20 | L26 | 3.81 | 0 | 44 | 55 |
| 136 | 34.30 | 3.70 | L23 | 3.89 | 94 | 5 | 5 |
| 137 | 14.31 | 2.30 | L13 | 2.70 | 99 | 2 | 1 |
| 138 | 14.31 | 3.50 | L28 | 3.03 | 101 | 0 | 0 |
| 139 | 14.31 | 3.40 | L26 | 2.76 | 10 | 43 | 48 |
| 140 | 14.31 | 2.10 | L23 | 2.38 | 95 | 4 | 5 |
| 141 | 14.31 | 2.30 | L28 | 2.43 | 104 | 0 | 1 |
| 142 | 14.31 | 3.30 | L31 | 3.09 | 84 | 9 | 11 |
| 143 | 14.31 | 3.40 | L12 | 3.18 | 1 | 2 | 94 |
| 144 | 14.31 | 2.20 | L14 | 2.64 | 11 | 2 | 86 |
| 145 | 15.40 | 5.00 | L13 | 2.00 | 49 | 25 | 25 |
| 146 | 15.40 | 3.60 | L14 | 2.67 | 5 | 3 | 90 |
| 147 | 15.40 | 3.30 | L30 | 2.73 | 52 | 35 | 14 |
| 148 | 15.40 | 2.60 | L26 | 1.31 | 10 | 39 | 52 |
| 149 | 15.40 | 3.40 | L26 | 2.94 | 4 | 48 | 51 |
| 150 | 15.40 | 2.30 | L23 | 1.30 | 76 | 12 | 23 |
| 151 | 15.40 | 3.90 | L16 | 1.38 | 16 | 5 | 78 |
| 152 | 15.40 | 3.80 | L28 | 2.47 | 100 | 1 | 0 |
| 153 | 39.60 | 2.80 | L28 | 3.93 | 90 | 6 | 3 |
| 154 | 39.60 | 3.50 | L23 | 3.94 | 93 | 3 | 6 |
| 155 | 39.60 | 1.50 | L16 | 2.80 | 64 | 8 | 27 |
| 156 | 39.60 | 3.40 | L16 | 2.41 | 30 | 12 | 57 |
| 157 | 39.60 | 1.10 | L13 | 3.82 | 102 | 0 | 0 |
| 158 | 39.60 | 1.30 | L26 | 3.85 | 11 | 42 | 48 |
| 159 | 39.60 | 2.90 | L30 | 4.00 | 2 | 74 | 28 |
| 160 | 39.60 | 3.30 | L26 | 3.82 | 1 | 45 | 54 |
| 161 | 27.71 | 3.00 | L14 | 3.73 | 10 | 4 | 85 |
| 162 | 27.71 | 3.20 | L23 | 3.75 | 93 | 3 | 5 |
| 163 | 27.71 | 3.10 | L26 | 3.48 | 1 | 46 | 53 |

| | | | | | | | |
|---|---|---|---|---|---|---|---|
| 164 | 27.71 | 3.30 | L31 | 3.70 | 91 | 17 | 3 |
| 165 | 27.71 | 4.10 | L32 | 1.56 | 49 | 24 | 25 |
| 166 | 27.71 | 4.10 | L17 | 1.46 | 44 | 20 | 33 |
| 167 | 27.71 | 1.20 | L23 | 3.33 | 96 | 2 | 4 |
| 168 | 27.71 | 4.10 | L13 | 1.51 | 32 | 30 | 37 |
| 169 | 23.43 | 3.70 | L4 | 3.68 | 97 | 1 | 4 |
| 170 | 23.43 | 3.50 | L28 | 1.94 | 95 | 2 | 1 |
| 171 | 23.43 | 3.30 | L26 | 2.36 | 0 | 45 | 54 |
| 172 | 23.43 | 3.20 | L14 | 2.31 | 4 | 4 | 92 |
| 173 | 23.43 | 2.60 | L23 | 1.62 | 92 | 3 | 7 |
| 174 | 23.43 | 5.00 | L30 | 1.60 | 11 | 61 | 27 |
| 175 | 23.43 | 3.80 | L24 | 2.05 | 46 | 23 | 29 |
| 176 | 23.43 | 3.70 | L25 | 3.68 | 88 | 3 | 7 |
| 177 | 18.35 | 4.90 | L18 | 1.06 | 26 | 15 | 57 |
| 178 | 18.35 | 5.00 | L27 | 1.12 | 4 | 5 | 88 |
| 179 | 18.35 | 4.70 | L23 | 2.94 | 94 | 2 | 5 |
| 180 | 18.35 | 5.00 | L22 | 1.04 | 45 | 20 | 33 |
| 181 | 18.35 | 5.00 | L13 | 0.84 | 14 | 25 | 57 |
| 182 | 18.35 | 3.90 | L26 | 0.51 | 5 | 24 | 70 |
| 183 | 18.35 | 4.80 | L19 | 0.96 | 10 | 26 | 64 |
| 184 | 18.35 | 4.90 | L22 | 1.06 | 47 | 20 | 32 |
| 185 | 21.54 | 4.70 | L22 | 1.53 | 46 | 19 | 33 |
| 186 | 21.54 | 4.70 | L22 | 1.53 | 46 | 19 | 33 |
| 187 | 21.54 | 1.60 | L32 | 1.13 | 69 | 15 | 18 |
| 188 | 21.54 | 4.60 | L18 | 1.26 | 28 | 17 | 54 |
| 189 | 21.54 | 4.70 | L22 | 1.53 | 42 | 19 | 35 |
| 190 | 21.54 | 4.70 | L22 | 1.53 | 45 | 19 | 33 |
| 191 | 21.54 | 1.30 | L16 | 1.38 | 24 | 4 | 71 |
| 192 | 21.54 | 1.80 | L26 | 0.78 | 10 | 32 | 60 |

## 6.7 Campaign 3 visualization

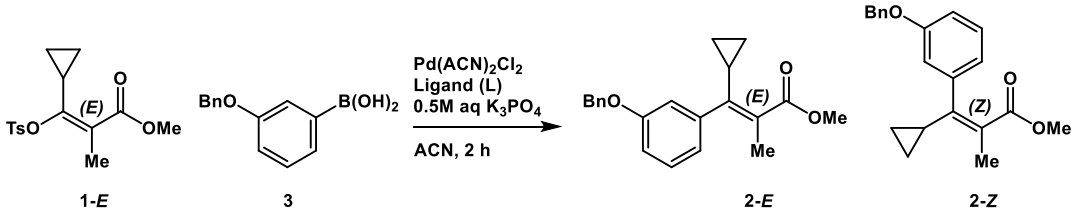


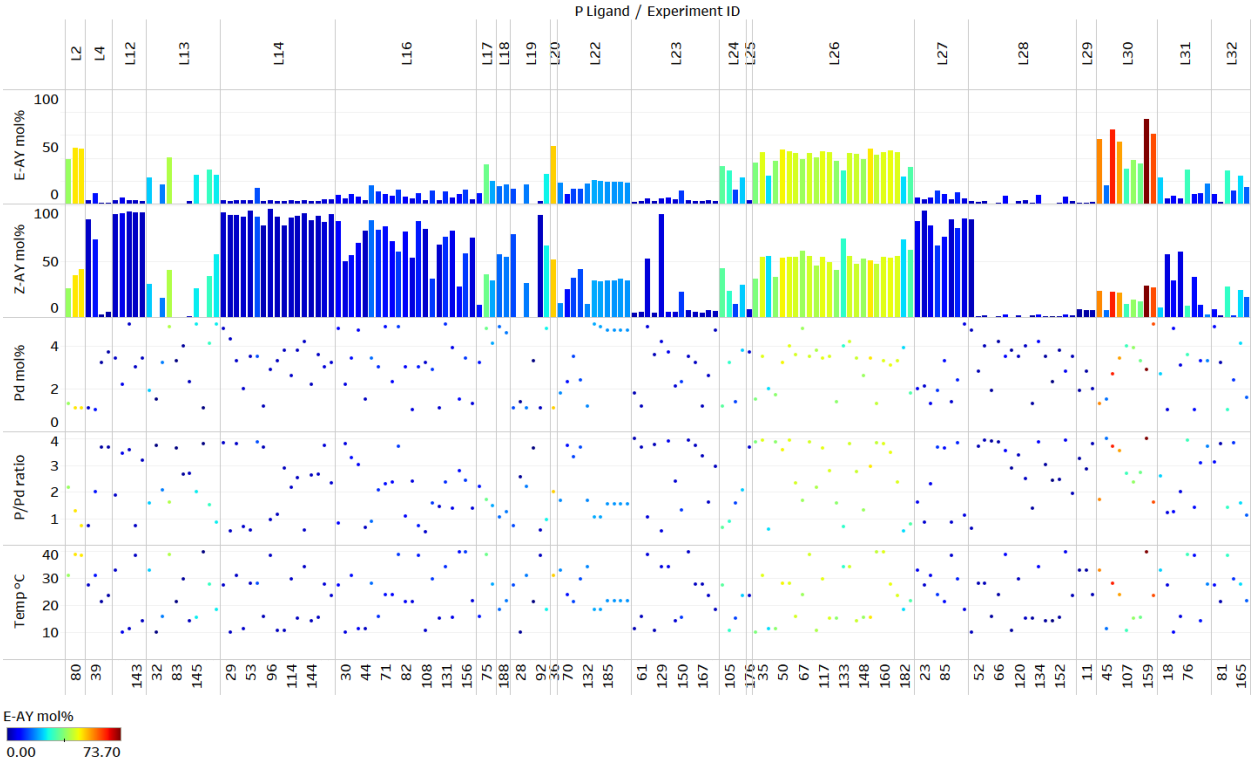


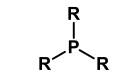

L13: R = Et
L14: R = Mesityl
L15: R = 3,5-Me-4-OMe-Ph
L16: R = nOctyl
L17: R = nPr

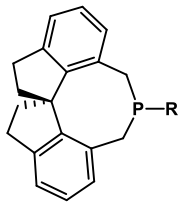

L18: (R)SITCP R = Ph

L19: R = Cy R'=Ph
L20: R = Ph R'=2,6-Me-Ph
L21: R = Ph R'=2-OMe-Ph
L22: R = Ph R' = Allyl
L23: R = $C_6F_5$ R'=Ph
L24: PhAtaPhos R = Ph R'= 4-$NMe_2$-Ph
L25: R = Ph R'= $(CH_2)_3Si(OEt)_3$
L26: R = 4-(2,2-$CF_3$-$F_7$pent)-Ph R'=Ph
L27: m-CroPhos R = tBu R'= *E*-butene

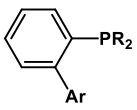

L28: R = Cy Ar = 2,4,6-OMe-Ph
L29: JohnPhos R = tBu Ar = Ph
L30: PhSPhos R= Ph Ar = 2,6-OMe-Ph
L31: SPhos R= Cy Ar = 2,6-OMe-Ph
L32: Et-PhenCarPhos R = Et Ar = Cz

**Figure SI-9. Parameters and results of optimization with ligands selected through descriptor clustering with 15 selected phosphine descriptors included in algorithmic optimization (campaign 3).**
Conditions: 10 µmol **1-*E***, 1 µmol 1,3,5-trimethoxybenzene, 15 µmol **3**, 0.1 - 0.5 µmol $Pd(ACN)_2Cl_2$, 0.05 - 2 µmol **L**, 30 µmol $K_3PO_4$ (0.5M aq) in ACN (0.05M), 2 h at 10 - 40 °C.

6.8 Standard experiments

In campaigns involving 192 iterations, two sets of eight standard experiments (conditions provided in Figure SI-10) were carried out in in each reaction block in order to measure reproducibility and system performance. We determined that the relative standard deviation (RSD) of measured **2-*E*** and **2-*Z*** yields fell between 6-8 %.

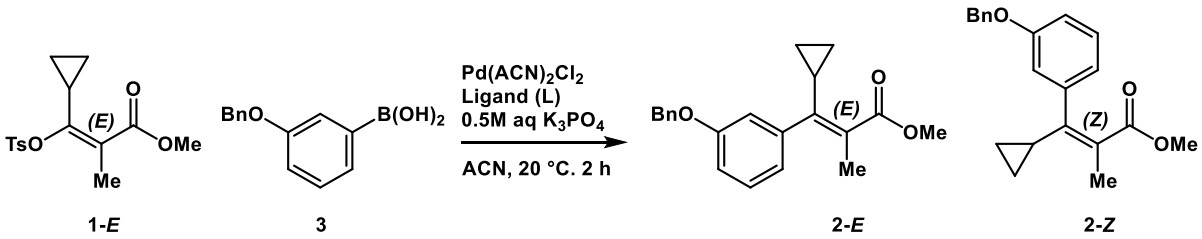


**Figure SI-10: Standard experimental conditions**
Conditions: 10 µmol **1-*E***, 1 µmol 1,3,5-trimethoxybenzene, 15 µmol **3**, 0.3 µmol $Pd(ACN)_2Cl_2$, 0.4 µmol **L2** ($PoTol_3$), 30 µmol $K_3PO_4$ (0.5M aq) in ACN (0.05M), 2 h at 20 °C.

**Table SI-13: Standard experiments from blocks 1 and 2 of campaign 2**

| Expt | Temp | Pd mol% | P ligand | P/Pd | 2-*E* mol% | 2-*Z* mol% |
|---|---|---|---|---|---|---|
| 1 | 20 | 2.5 | L2 | 1.52 | 34 | 22 |
| 2 | 20 | 2.5 | L2 | 1.52 | 32 | 20 |
| 3 | 20 | 2.5 | L2 | 1.52 | 28 | 17 |
| 4 | 20 | 2.5 | L2 | 1.52 | 31 | 19 |
| 5 | 20 | 2.5 | L2 | 1.52 | 30 | 19 |
| 6 | 20 | 2.5 | L2 | 1.52 | 28 | 17 |
| 7 | 20 | 2.5 | L2 | 1.52 | 30 | 18 |
| 8 | 20 | 2.5 | L2 | 1.52 | 31 | 19 |
| **Average** | | | | | **30** | **19** |
| **SD** | | | | | **2** | **1** |
| **RSD%** | | | | | **6** | **8** |
| 97 | 20 | 2.5 | L2 | 1.52 | 28 | 17 |
| 98 | 20 | 2.5 | L2 | 1.52 | 31 | 18 |
| 99 | 20 | 2.5 | L2 | 1.52 | 30 | 18 |
| 100 | 20 | 2.5 | L2 | 1.52 | 28 | 17 |
| 101 | 20 | 2.5 | L2 | 1.52 | 25 | 15 |
| 102 | 20 | 2.5 | L2 | 1.52 | 27 | 16 |
| 103 | 20 | 2.5 | L2 | 1.52 | 28 | 17 |
| 104 | 20 | 2.5 | L2 | 1.52 | 28 | 18 |
| **Average** | | | | | **28** | **17** |
| **SD** | | | | | **2** | **1** |
| **RSD%** | | | | | **6** | **6** |

## 7. Predictive model

Multivariate linear regression (MLR) was employed to generate a predictive model for yield of product **2-*E*** based on the highest yield of **2-*E*** per ligand in any experiment in campaigns 2 and 3. The model is shown below.

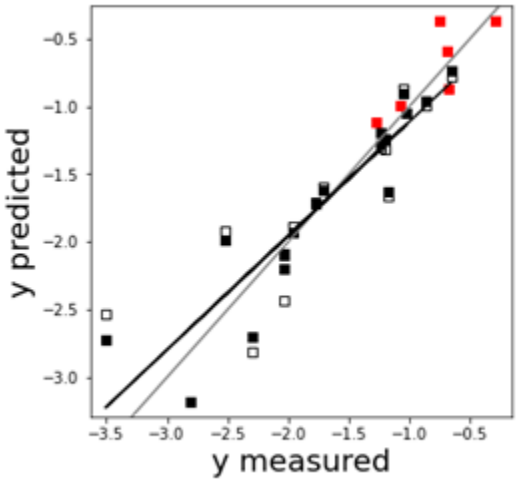


| p-value | coefficient | |
|---|---|---|
| 1.32E-10 | -1.7133 + | |
| 2.73E-04 | -2.6077 * x5 fmo_mu_boltz | (HOMO-LUMO gap) |
| 1.34E-03 | -2.1383 * x7 fmo_omega_boltz | (electrophilicity-index) |
| 1.32E-05 | 1.0014 * x30 nbo_bds_e_min_boltz | (Energy of lowest P-C antibonding orbital) |
| 3.35E-04 | -0.7124 * x98 vbur_qvtot_min_boltz | (volume of the smallest ligand quadrant) |

Training $R^2$ = 0.844
Training $Q^2$ = 0.747
Training MAE = 0.200
Training K-fold $R^2$ = 0.703 (+/- 0.005)
Test $R^2$ = 0.958
Test MAE = 0.169

**Figure SI-11. Multivariate regression model generated from campaign 2 and 3 data.**
Note: y is the ln of the highest yield of **2-*E*** per ligand in any experiment.

---

[1] This compound was previously characterized in Christensen, M. *et al.* Enantioselective synthesis of α-methyl-β-cyclopropyldihydrocinnamates. *J. Org. Chem.* **81,** (2016).
[2] This compound was previously characterized in Christensen, M. *et al.* Development of an automated kinetic profiling system with online HPLC for reaction optimization. *React. Chem. Eng.* **4,** 1555–1558 (2019).

[3] This compound was previously characterized in Li, Y., Das, S., Zhou, S., Junge, K. & Beller, M. General and selective copper-catalyzed reduction of tertiary and secondary phosphine oxides: Convenient synthesis of phosphines. *J. Am. Chem. Soc.* **134,** 9727–9732 (2012).

[4] Häse, F., Roch, L. M., Kreisbeck, C. & Aspuru-Guzik, A. Phoenics: A Bayesian Optimizer for Chemistry. *ACS Cent. Sci.* **4,** 1134–1145 (2018).

[5] Häse, F., Roch, L. M. & Aspuru-Guzik, A. Gryffin: An algorithm for Bayesian optimization for categorical variables informed by physical intuition with applications to chemistry. (2020).

[6] Algorithm 1 reported in Vellanki, P. *et al.* Process-constrained batch Bayesian Optimisation. (2017).